

METHODOLOGICAL NOTES

PACS numbers: **41.60. – m**, **52.35. – g**, 52.40.Mj

ON THE 270th ANNIVERSARY OF M.V. LOMONOSOV MOSCOW STATE UNIVERSITY (MSU)

Stimulated Cherenkov effect and dissipative-radiative instabilities in superluminal motion of a relativistic electron beam in a layered medium

M.V. Kuzelev

DOI: https://doi.org/10.3367/UFNe.2025.01.039850

Contents

Abstract. Dissipative–radiative instabilities and instabilities caused by the stimulated Cherenkov effect of a relativistic electron beam in an unbounded layered electrodynamic system are considered. While for the stimulated Cherenkov effect the beam energy is used to excite waves in the electrodynamic system, for dissipative–radiative instabilities, the beam energy is radiated away from the system to infinity. Such irreversible energy transfer from the beam manifests itself as a kind of effective dissipation and makes the dissipative–radiative instability an analogue of the usual dissipative beam instability in a system without radiation. Growth rates and frequency ranges of the instabilities are found for various structures of layered electrodynamic systems, including plasma systems.

Keywords: relativistic electron beams, stimulated Cherenkov effect, dissipative–radiative instability

1. Introduction

The stimulated Cherenkov effect is an instability in which an electron beam excites (causes the emission of) an eigenwave in an electrodynamic system under the conditions of Cherenkov resonance. In a linear approximation, the stimulated Cherenkov effect is described by the dispersion equation [1, 2]

$$D_0(\omega, k_z) - \alpha(\omega, k_z)\,\frac{\omega_b^2}{(\omega - k_z u)^2} = 0\,, \tag{1}$$

where $D_0(\omega, k_z)$ is the dispersion function of the electrodynamic system in which the beam propagates, ω_b is the Langmuir frequency of the beam electrons, u is the beam velocity, k_z is the projection of the wave vector onto the beam motion direction, and $\alpha(\omega, k_z)$ is a function without zeros and singularities. The eigenfrequency of the electrodynamic system is obtained from the equation $D_0(\omega, k_z) = 0$, which, under the Cherenkov resonance condition $\omega = k_z u$, gives the equation for the resonance wavenumber:

$$D_0(k_z u, k_z) = 0 \to k_z = k_{z0}\,. \tag{2}$$

The resonance frequency is defined as $\omega_0 = k_{z0}u$. A necessary condition for the existence of the stimulated Cherenkov effect is that there be real solutions of equation (2). The instability increment in the stimulated Cherenkov effect has a pronounced resonance shape, reaching a maximum at $k_z = k_{z0}$. The lower the beam density, the sharper the resonance. The maximum increment is easily calculated from equation (1) by substituting $\omega = \omega_0 + \delta\omega$ and $k_z = k_{z0}$, which gives

$$\delta\omega(k_{z0}) = \frac{-1 + i\sqrt{3}}{2}\left[\alpha(\omega_0, k_{z0})\left(\frac{\partial D_0}{\partial \omega}\right)^{-1}\omega_b^2\right]^{1/3}, \tag{3}$$

where the derivative of $D_0(\omega, k_z)$ with respect to frequency is taken at the resonance point ω_0, k_{z0}. To obtain expression (3), it was assumed that $|\delta\omega| \ll \omega_0$.

M.V. Kuzelev
Lomonosov Moscow State University, Faculty of Physics,
Leninskie gory 1, str. 2, 119991 Moscow, Russian Federation
E-mail: kuzelev@mail.ru

Received 3 March 2024, revised 27 January 2025
Uspekhi Fizicheskikh Nauk **195** (4) 432 – 449 (2025)
Translated by S.D. Danilov

Far from the point of the Cherenkov resonance or when the Cherenkov resonance is impossible, i.e., when equation (2) has no real solutions, equation (1) defines the frequencies of the waves of the beam spatial charge — the fast wave and the slow wave [3, 4]. Under the inequality $\omega_b \ll k_z u$, equation (1) gives for the frequencies of such waves

$$\omega(k_z) = k_z u \pm \sqrt{\frac{\alpha(k_z u, k_z)}{D_0(k_z u, k_z)}}\,\omega_b\,. \tag{4}$$

Note that there are systems with $\alpha/D_0 < 0$. In this case, the frequencies (4) are complex, and the imaginary part of one of them is positive. This is a case of the negative mass instability type of so-called aperiodic instability [5]. An example is the long-wave instability of an unbounded monovelocity electron beam in a cold unbounded plasma [6].

In the presence of dissipative effects, the dispersion function becomes complex:

$$D_0(\omega, k_z) = D_0'(\omega, k_z) + \mathrm{i}D_0''(\omega, k_z)\,.$$

If the dissipation is weak, it can be disregarded when considering the stimulated Cherenkov effect, i.e., when calculating the increment (3). However, for the waves of the beam charge density, the imaginary part of the dispersion function in formula (4) cannot be neglected, however small it may be. It is related to an effect called dissipative beam instability [7]. Unlike the stimulated Cherenkov effect, the dissipative beam instability is not related to the excitation by the beam of some eigenwaves in the system in which the beam propagates. Instead, it is the waves of the beam itself (4) that are excited. One of the electron beam waves, namely the slow spatial charge wave, has a negative energy, i.e., to excite this wave, energy is taken from the beam [8, 9]. Thus, if there is a channel to remove the energy, a perturbation in the beam will spontaneously grow. For the dissipative beam instability, such a channel is the dissipation of electromagnetic energy in the medium. This is essentially the mechanism of dissipative beam instability. In microwave (MW) electronics, the dissipative beam instabilities are known as the effect of gain on absorption [10]. If the inequality

$$\left|D_0''(k_z u, k_z)\right| \ll \left|D_0'(k_z u, k_z)\right|$$

holds, then, for the imaginary part of formula (4), we have

$$\delta\omega(k_z) = \pm\mathrm{i}\,\frac{1}{2}\sqrt{\frac{\alpha(k_z u, k_z)}{D_0'(k_z u, k_z)}}\,\frac{D_0''(k_z u,\, k_z)}{D_0'(k_z u,\, k_z)}\,\omega_b\,. \tag{5}$$

One of the values in (5) defines the instability increment (growth rate). The dissipative instability is not a resonance instability, and consequently its increment is weakly dependent on the wave number k_z.

There is another important mechanism for removing electromagnetic energy from the system, namely radiation. In any unbounded electrodynamic system, there is necessarily a channel that allows energy to escape as radiation. Loss of energy by radiation is equivalent to some dissipation. It does not matter for the beam whether the energy is removed by dissipation or by radiation. Therefore, when an electron beam passes through an electrodynamic system with radiation, the negative energy wave can be spontaneously amplified in it, as in a normal dissipative system. In this case, the released beam energy is carried to infinity by radiation. Such an instability is called here a dissipative–radiative beam instability, or gain on radiation (by analogy with gain on absorption).

Below we consider an unbounded layered electrodynamic system penetrated by an electron beam propagating parallel to layer interfaces. The outer layers in this system are extended to infinity. As is well known, to obtain the dispersion function of a layered electrodynamic system, a general solution of the electromagnetic field equations is written in each layer, and these solutions are then matched at the layer interfaces. Solutions of the field equations for semi-bounded layers (with one boundary at infinity), describing waves propagating (emitted) to infinity, are expressed in terms of complex-valued functions. For example, in a plane geometry, they are $\exp(\pm\mathrm{i}k_x x)$, while in the cylindrical geometry they are the Hankel functions $H_0^{(1)}(k_r r)$, where k_x and k_r are the wave numbers of the respective directions. Therefore, the dispersive function $D_0(\omega, k_z)$ of an unbounded layered system is a complex-valued function of real frequency ω and real wavenumber k_z, just as in a bounded dissipative system. Accordingly, the dispersion equation describing the excitation of an electrodynamic system with radiation by a beam has the structure of the dispersion equation for charge density waves in a dissipative system. The increment of the dissipative–radiative instability has the same structure as (5), i.e., it depends only weakly on the wave number k_z. The dissipative–radiative instability is nonresonant.

The similarity of dissipative and dissipative–radiative instabilities is also evident from the following considerations. In electrodynamics, instead of radiation conditions at infinity,[1] the well-known Leontovich boundary conditions [12] are often applied by introducing a fictive (or actually existing) boundary with a medium that absorbs electromagnetic waves (see also Fig. 1). The dispersion function $D_0(\omega, k_z)$ becomes complex due to the Leontovich conditions, and real dissipation is added to the electrodynamic system.

Let us make an important clarification that applies equally to both the dissipative and the dissipative–radiative instabilities. Previously, when deriving formula (5), we used the inequality

$$\left|D_0''(k_z u, k_z)\right| \ll \left|D_0'(k_z u, k_z)\right|,$$

which implies not only that the dissipation is small, but also that the Cherenkov resonance is absent, i.e., $D_0'(k_z u, k_z) \neq 0$. If in a dissipative system the Cherenkov resonance condition $D_0'(k_z u, k_z) = 0$ is observed for some value of k_z, it is more relevant to relate the instability to the stimulated Cherenkov effect in a dissipative system [13] than to a dissipative instability. Further, when classifying beam instabilities, we will use the terms dissipative–radiative instability and gain on radiation only when the stimulated Cherenkov effect is impossible.

Note that, despite all the formal similarities between dissipative and dissipative–radiative instabilities, there is an important distinction. In a dissipative beam instability, the kinetic energy of the beam is converted into heating of the medium in which the beam propagates. In the dissipative–radiative instability, the kinetic energy of the beam is converted into the energy of electromagnetic waves emitted by the system. In terms of their outcome, the dissipative–radiative instabilities have much in common with radiative instabilities in stimulated Cherenkov effects. In limiting cases,

[1] Sommerfeld's conditions [11] are meant.

the increments of beam instabilities listed here are governed by different expressions, their mechanisms have a different physical nature, and the results of their development prove to be different, but the instabilities manifest themselves in electrodynamic structures of a similar geometry and in conditions similar to those of the Cherenkov resonance ($\omega \approx k_z u$). It is important to distinguish and strictly classify such instabilities, as they define the dynamics of high-frequency electromagnetic processes accompanying the propagation of electron beams in retarding systems, e.g., in electrodynamic systems of plasma and vacuum MW electronics.

2. Dispersion equation

Consider a layered system consisting of an unbounded isotropic dielectric with permittivity ε_0 containing a channel with flat boundaries at $x = -L$ and $x = +L$, filled with a homogeneous medium with the dielectric permittivity tensor

$$\varepsilon_{ij}(\omega) = \begin{pmatrix} \varepsilon_\perp(\omega) & 0 & 0 \\ 0 & \varepsilon_\perp(\omega) & 0 \\ 0 & 0 & \varepsilon_\parallel(\omega) \end{pmatrix}, \quad i, j = x, y, z, \qquad (6)$$

where $\varepsilon_\perp$ and $\varepsilon_\parallel$ are some functions of frequency. A thin ribbon monovelocity electron beam propagates along the channel, in the direction of the z-axis. We express the Langmuir frequency of the electrons in this beam as

$$\omega_b^2(x) = \omega_{b0}^2 \Delta_b \delta(x), \qquad (7)$$

where ω_{b0}^2 is a constant, Δ_b is the beam thickness, and $\delta(x)$ is the delta function. The quantity $\omega_{b0}^2 \Delta_b$ is proportional to the line density of the electrons in the beam. This is the quantity with which experimenters working with narrow ribbon and tubular beams are concerned. The beam is assumed to be fully magnetized by a strong external magnetic field directed along the z-axis.[2]

The layered system with an electron beam, which is described above, and also two other layered systems of interest are shown in Fig. 1; the beam is shown in red. In this study, it is assumed that the absorbers, shown in the figure, are at infinity, which would correspond to the limits $L_\infty \to \infty$ in Fig. 1a and $R_\infty \to \infty$ in Fig. 1b. It should be obvious that the cases with absorbers at a finite or infinite distance from the beam are physically equivalent (see above). The plane layered system (Fig. 1a) is mainly of theoretical interest due to the relative simplicity of its analysis. A more practically important cylindrical system (Fig. 1b, a tubular beam propagating perpendicularly to the plane of the figure) is considered in Section 6. The system shown in Fig. 1c (a needle beam propagating perpendicularly to the plane of the figure) is not considered in this paper but is undoubtedly a system with dissipative–radiative instability and is of certain interest for applications as well as for the theory of waves in nonequilibrium inhomogeneous media.

We continue with the system shown in Fig. 1a. Since the parameters of our layered system depend only on the

[2] For beams with a small cross section, their transverse polarization is not essential; it is the longitudinal polarization that determines their behavior. Therefore, the requirement of magnetization when describing high-frequency processes for a thin ribbon electron beam is, generally speaking, not necessary [14]. The magnetization of the electron beam, especially at high density, is important for its transport.

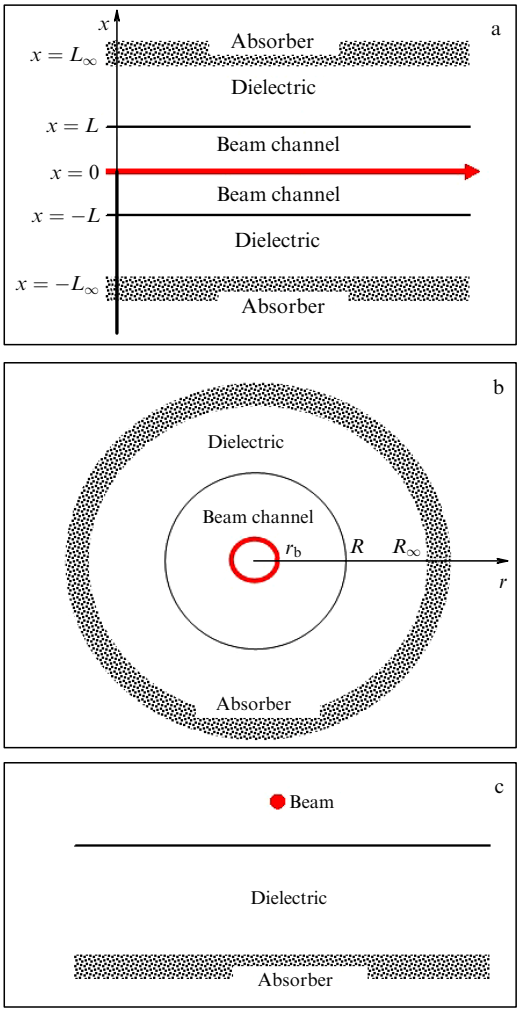

Figure 1. Layered systems supporting dissipative–radiative instabilities: (a) plane system; (b) cylindrical system; (c) beam over flat surface.

coordinate x, the electromagnetic field components are sought in the form

$$f(x) \exp(-i\omega t + ik_z z). \qquad (8)$$

For fields that can be written in the form of (8), Maxwell's equations are split into two independent subsystems for the components E_z, E_x, B_y (E-type) and the components B_z, B_x, E_y (B-type). Here, we are only interested in the subsystem for E-type waves, which for complex field amplitudes is written as

$$\begin{aligned} ik_z E_x - \frac{dE_z}{dx} &= i\frac{\omega}{c} B_y, \\ k_z B_y &= \frac{\omega}{c} \varepsilon_{xx}(x) E_x, \\ \frac{dB_y}{dx} &= -i\frac{\omega}{c}\left[\varepsilon_{zz}(x) + \delta\varepsilon_b(x)\right] E_z. \end{aligned} \qquad (9)$$

Here,

$$\varepsilon_{xx}(x) = \begin{cases} \varepsilon_\perp, & |x| < L, \\ \varepsilon_0, & |x| > L, \end{cases} \quad \varepsilon_{zz}(x) = \begin{cases} \varepsilon_\parallel, & |x| < L, \\ \varepsilon_0, & |x| > L, \end{cases}$$
$$\delta\varepsilon_b(x) = -\frac{\omega_b^2(x)\gamma^{-3}}{(\omega - k_z u)^2}. \qquad (10)$$

The beam contribution to the dielectric permittivity $\delta\varepsilon_b$ is calculated here in the hydrodynamic approximation [15], and $\gamma = (1 - u^2/c^2)^{-1/2}$ is the relativistic factor of a beam electron.[3]

Excluding the electromagnetic field components E_x and B_y from system (9), we obtain the following equation for the electric field component E_z:

$$\frac{\mathrm{d}}{\mathrm{d}x}\left(\frac{\varepsilon_{xx}(x)}{\chi_{xx}^2(x)}\,\frac{\mathrm{d}E_z}{\mathrm{d}x}\right) = \left[\varepsilon_{zz}(x) + \delta\varepsilon_b(x)\right]E_z\,, \tag{11}$$

where $\chi_{xx}^2(x) = k_z^2 - \varepsilon_{xx}(x)\omega^2/c^2$. Integrating equation (11) over an infinitely small vicinity of $x = 0$ and taking into account (7), (10) and the continuity of the function $E_z(x)$, we obtain a constraint on the jump of the derivative of $E_z(x)$ at the point where the electron beam passes,

$$\left\{\frac{\mathrm{d}E_z}{\mathrm{d}x}\right\}_{x=0} = -\Delta_b\chi_\perp^2\,\frac{\omega_{b0}^2\gamma^{-3}}{\varepsilon_\perp(\omega - k_z u)^2}\,E_z(0)\,,\quad \chi_\perp^2 = k_z^2 - \frac{\omega^2}{c^2}\,\varepsilon_\perp\,, \tag{12}$$

where the notation $\{f(x)\}_{x=a} = f(a+0) - f(a-0)$ has been used. In addition, at the boundaries of the dielectric $x = \pm L$, the following continuity conditions should be satisfied:[4]

$$\left\{E_z(x)\right\}_{x=\pm L} = 0\,,\quad \left\{\frac{\varepsilon_{xx}(x)}{\chi_{xx}^2(x)}\,\frac{\mathrm{d}E_z}{\mathrm{d}x}\right\}_{x=\pm L} = 0\,. \tag{13}$$

In addition to conditions (12) and (13), we also consider the symmetry of the layered system under consideration here with respect to the point $x = 0$, which implies that the function $E_z(x)$ can be either odd or even. Since $E_z(x)$ is continuous at the zero argument, then, if it is odd, it must satisfy $E_z(0) = 0$, and this case is of no interest due to condition (12). We therefore assume that the function $E_z(x)$ is even, which can be conveniently written as

$$\left.\frac{\mathrm{d}E_z}{\mathrm{d}x}\right|_{x=-0} = -\left.\frac{\mathrm{d}E_z}{\mathrm{d}x}\right|_{x=+0}\,. \tag{14}$$

Given (14), we can restrict ourselves to $x > 0$ when solving equation (11).

A solution of equation (11) in the region $(0, L)$ is given by the expression

$$E_z = A\exp(-\kappa x) + B\exp(\kappa x)\,, \tag{15}$$

where A and B are constants and $\kappa = \sqrt{\chi_\perp^2\varepsilon_\parallel/\varepsilon_\perp}$. In the region (L, ∞), the solution should describe a wave traveling to infinity, but only in the case where the wave is propagating or emitted. When the wave is evanescent, it should decay exponentially at infinity. The solution that satisfies these requirements is of the form [16]

$$E_z = C\exp(\xi x)\,,\qquad \xi = \begin{cases} \mathrm{i}\kappa_0\,, & \operatorname{Re}\kappa_0^2 > 0\,,\\ -\chi_0\,, & \operatorname{Re}\kappa_0^2 < 0\,, \end{cases} \tag{16}$$

where

$$\kappa_0^2 = \frac{\omega^2}{c^2}\,\varepsilon_0 - k_z^2\,,\quad \chi_0^2 = -\kappa_0^2\,. \tag{17}$$

In writing solutions (15) and (16), we have taken into account the first two formulas (10). Note that we are following the conventional rule for the square root of a complex quantity, according to which the branch with a positive real part is chosen.

Inserting solutions (15) and (16) into the matching conditions (12) and (13) and taking into account relationship (14), we obtain a linear homogeneous system of algebraic equations on the constants A, B, and C. Its solvability condition — the requirement that its determinant be zero — leads to the following dispersion equation, which governs the frequency spectra in the layered electrodynamic system with the ribbon beam studied here,

$$\frac{(\varepsilon_\perp\kappa\chi_0^2 - \varepsilon_0\xi\chi_\perp^2) - (\varepsilon_\perp\kappa\chi_0^2 + \varepsilon_0\xi\chi_\perp^2)\exp(-2\kappa L)}{(\varepsilon_\perp\kappa\chi_0^2 - \varepsilon_0\xi\chi_\perp^2) + (\varepsilon_\perp\kappa\chi_0^2 + \varepsilon_0\xi\chi_\perp^2)\exp(-2\kappa L)} = \frac{1}{2}\,\Delta_b\,\frac{\chi_\perp^2}{\kappa\varepsilon_\perp}\,\frac{\omega_{b0}^2\gamma^{-3}}{(\omega - k_z u)^2}\,. \tag{18}$$

Equation (18) has the form of the dispersion equation (1). The left-hand side of (18), more precisely its numerator, is the dispersion function $D_0(\omega, k_z)$ of a plane Fabry–Pérot resonator formed by the medium in the channel $-L < x < L$ in the dielectric. In the dielectric half-spaces $x < -L$ and $x > L$, there are propagating waves that carry energy away from the resonator. Equation (18) will be explored further for three particular cases of the channel in the dielectric, namely, a vacuum channel, a channel with isotropic plasma, and a channel with a highly anisotropic plasma.

3. Dissipative–radiative instability in vacuum channel

For a vacuum channel in a dielectric, we should use $\varepsilon_\perp = \varepsilon_\parallel = 1$ in equation (18). In this case, $\chi_\perp^2 = k_z^2 - \omega^2/c^2$, $\kappa = \sqrt{\chi_\perp^2}$. Before embarking on a full analysis, let us consider equation (18) in two limit cases, which are important for what follows. For $\omega_{b0}^2\Delta_b = 0$, i.e., in the absence of the beam, equation (18) is reduced, using notations adopted earlier, to the following equation:

$$\begin{aligned} D_0(\omega, k_z) = {} & \left(\varepsilon_0\sqrt{\frac{\omega^2}{c^2} - k_z^2} - \sqrt{\varepsilon_0\frac{\omega^2}{c^2} - k_z^2}\right)\\ & - \left(\varepsilon_0\sqrt{\frac{\omega^2}{c^2} - k_z^2} + \sqrt{\varepsilon_0\frac{\omega^2}{c^2} - k_z^2}\right)\\ & \times\exp\left(-2\mathrm{i}\sqrt{\frac{\omega^2}{c^2} - k_z^2}\,L\right) = 0\,. \end{aligned} \tag{19}$$

Equation (19) defines the discrete eigenfrequencies of a vacuum Fabry–Pérot resonator formed by flat interfaces $x = \pm L$. The solutions of equation (19) can be written approximately as

$$\begin{aligned} &\operatorname{Re}\omega \approx \sqrt{k_{\perp n}^2c^2 + k_z^2c^2}\,,\quad k_{\perp n} = \frac{\pi(n + 1/2)}{L}\,,\quad n = 0, 1, \ldots,\\ &\operatorname{Im}\omega \approx \frac{c}{2L}\ln\frac{\sqrt{\varepsilon_0} - 1}{\sqrt{\varepsilon_0} + 1} < 0\,. \end{aligned} \tag{20}$$

[3] When writing equation (4) earlier, we assumed that the beam is nonrelativistic, and therefore took $\gamma = 1$.

[4] Condition (12) defines the jump of the magnetic field component B_y on the current of an infinitely thin beam. The second condition (13) implies the continuity of B_y at the interface between the media. It follows directly from equation (11).

Solution (20) is exact only for $k_z = 0$, but, even for a finite k_z, it correctly models the dispersion law for the eigenwaves of the vacuum resonator. The imaginary part of frequencies (20) is due to waves $\exp(\pm ik_x x)$ propagating to infinity, where $k_x = \sqrt{\varepsilon_0\omega^2/c^2 - k_z^2}$. They are not eigenwaves because, as could be seen from formulas (20), there are no such eigenwaves in the system. They are excited by the eigenwaves through the channel boundaries at $x = \pm L$.

The second limit form of (18), which is important for further discussion, is obtained by setting $\varepsilon_0 = 1$ or letting L go to infinity (and considering $\chi_\perp^2 > 0$). In this limit, equation (18) gives

$$(\omega - k_z u)^2 = \frac{1}{2}\Delta_b\sqrt{k_z^2 - \frac{\omega^2}{c^2}}\,\omega_{b0}^2\gamma^{-3}. \tag{21}$$

Equation (21) defines the frequencies of the fast and slow waves of the charge density of a ribbon beam in a vacuum. The equation can be easily solved if the electron beam density is low. In this case, using the perturbation method,[5] one can insert $\omega = k_z u$ into the right-hand side of this equation. For the frequencies of the charge density waves, this gives

$$\omega = k_z u \pm \sqrt{\frac{1}{2}\Delta_b k_z}\,\omega_b\gamma^{-2}. \tag{22}$$

If the beam density is not low, the frequencies of the fast and slow charge density waves are no longer symmetric relative to the line $\omega = k_z u$. Furthermore, solution (22) is only valid under the condition that the second term on its right-hand side be small compared to the first. It is obvious that this condition is violated as k_z decreases. In the following, we will consider only low-density electron beams, when the above complications for the spectra of the waves of the beam charge density can be ignored.

The structure of the wave field of the beam charge density waves is described by the functions $\exp(\pm\sqrt{k_z^2 - \omega^2/c^2}\,x)$. The 'plus' sign is used for $x < 0$, and the 'minus' sign for $x > 0$. In the case of a low density beam, these functions are reduced to $\exp(\pm k_z\gamma^{-1}x)$. Thus, the beam charge density waves are surface waves over the coordinate x.

An instability of the stimulated Cherenkov effect is impossible in the Fabry–Pérot resonator considered here. Indeed, the phase velocity of waves (20) is greater than the speed of light in a vacuum, and therefore the equation $D_0(k_z u, k_z) = 0$, where the dispersion function D_0 is defined by (19), has no solutions. This seems to lead to an unequivocal conclusion: an electron beam propagating in a vacuum channel in an unbounded isotropic dielectric is stable. However, this conclusion is only valid for $u < c/\sqrt{\varepsilon_0}$. If an opposite inequality holds, an instability arises, as we will now see. A legitimate question here is why the medium with dielectric permittivity ε_0 matters. In fact, there are no eigenwaves with the phase velocity $c/\sqrt{\varepsilon_0}$ in the resonator, and the beam propagates in the vacuum channel, not in a medium. It's all about the charge density waves. The fields of these waves induce electric charges at a frequency close to $k_z u$ at the boundaries of the medium with dielectric permittivity ε_0. These charges excite electromagnetic waves which propagate to infinity in regions $|x| > L$. The condition for the excitation of such outgoing waves is namely the inequality $u > c/\sqrt{\varepsilon_0}$. The wave propagating to infinity is given by formula (16). Such a wave is not an eigenwave of the electrodynamic system considered here, but it is a real wave that is excited, takes energy from the beam, and carries it to infinity.

It is obvious that, to realize the process described above, the channel $|x| < L$ in the medium with dielectric permittivity ε_0 is not actually needed. The channel largely allows for beam transport. One can arrive at a case where the channel is absent if in the original dispersion equation (18) (before $\varepsilon_\perp$ and $\varepsilon_\parallel$ are replaced by unity) one takes $\varepsilon_\perp = \varepsilon_\parallel = \varepsilon_0$ or assumes that L tends to zero. As a result of such actions, equation (18) is reduced to the following equation:

$$(\omega - k_z u)^2 = \frac{1}{2}\Delta_b\sqrt{k_z^2 - \frac{\varepsilon_0\omega^2}{c^2}}\,\frac{\omega_{b0}^2\gamma^{-3}}{\varepsilon_0}. \tag{23}$$

The main difference between equation (23) and the analogous equation (21) is that, instead of $\sqrt{k_z^2 - \omega^2/c^2}$, the former contains $\sqrt{k_z^2 - \varepsilon_0\omega^2/c^2}$. Since, for waves of beam charge density, $\omega \approx k_z u$, then, under the condition $u > c/\sqrt{\varepsilon_0}$, one can write the approximation

$$\sqrt{k_z^2 - \frac{\varepsilon_0\omega^2}{c^2}} \approx -ik_z\sqrt{\frac{\varepsilon_0 u^2}{c^2} - 1} \approx -i\left(\frac{\omega}{u}\right)\sqrt{\frac{\varepsilon_0 u^2}{c^2} - 1}. \tag{24}$$

Here, when taking the square root, we have taken into account that the frequency ω has a positive imaginary part. As a result, for a low density beam, the solution to equation (23) can be written as

$$\omega(k_z) = k_z u + \frac{1}{2}(-1 + i)\sqrt{\Delta_b k_z\sqrt{\frac{\varepsilon_0 u^2}{c^2} - 1}}\,\frac{\omega_{b0}\gamma^{-3/2}}{\sqrt{\varepsilon_0}}. \tag{25}$$

The positive imaginary part of frequency (25) is the instability growth rate. The question arises as to how such an instability should be classified. It cannot be treated as a stimulated Cherenkov effect, because the layered system considered here does not support eigenwaves that are in Cherenkov resonance with the beam (the equation $D_0(k_z u, k_z) = 0$, where D_0 is defined by (19), has no solutions[6]). In addition, equation (23) has nothing in common with the 'canonic' dispersion equation (1) for the stimulated Cherenkov effect, while the growth rate in formula (25) has a cardinally different structure from the increment (3). The fact that dispersion equations (1) and (23) describe different physical processes is well seen when we go to the limit $\omega_b^2 \to 0$ in these equations. Equation (1) in this limit gives an equation for the frequency spectra of the eigenwaves of the system, and equation (23) for $\omega_b^2 = 0$ gives only a single-particle spectrum $\omega = k_z u$. And this should be clear, since there are no eigenwaves in a half-space (unless they come from infinity).[7] There are only induced waves, which are excited and supported by the electron beam at $x = 0$ and leave towards infinity, carrying with them the energy used to excite them. One can therefore draw a clear conclusion: the beam instability described by dispersion equation (23) should be classified as dissipative–radiative, or the effect of gain on radiation.

Consider also the results of the numerical solution of dispersion equation (23), and also, for comparison, equa-

[5] Solutions (4) and (5) were obtained in exactly the same way.

[6] For $L = 0$, this equation is reduced to $k_z\sqrt{\varepsilon_0 u^2/c^2 - 1} = 0$.

[7] In an unbounded space, eigenwaves are undoubtedly possible. They come from infinity of one sign and continue to infinity of the other sign.

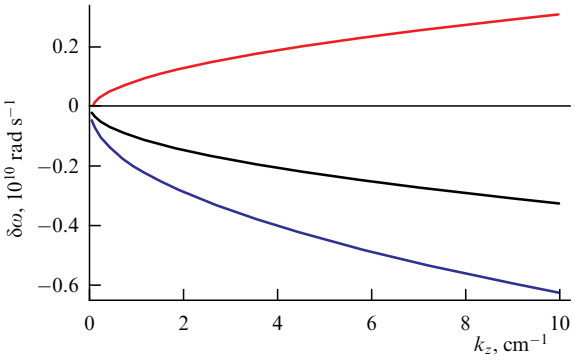

Figure 2. Complex increment of dissipative–radiative instability (Im ω is red and Re ω is black) and correction to slow wave frequency (blue).

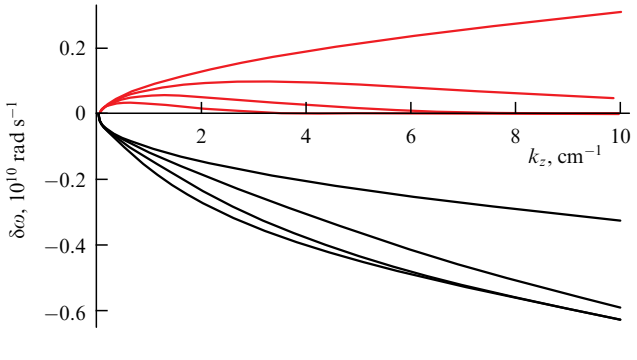

Figure 4. Complex increment of dissipative–radiative instability for a beam propagating in a vacuum channel: Im $\delta\omega$ (red), Re $\delta\omega$ (black), $L = 0$, 0.2, 0.5, 1 cm (from top downward).

tion (21). Figure 2 shows, for a beam with a current of 100 A[8] propagating at a speed of $u = 2.5 \times 10^{10}$ cm s^{-1} in a medium with dielectric permittivity $\varepsilon_0 = 2$, the quantity $\delta\omega = \omega - k_z u$, which is a complex increment[9] of the dissipative–radiative instability, as a function of k_z. The same figure shows the real quantity $\delta\omega$ in the slow charge density wave of the same beam, but propagating in a vacuum, found by the numerical solution of (21). Since the beam density is not high, the curves shown in Fig. 2 are well described by the second formula (21) and formula (25).

The structure of the wave field of the dissipative–radiative instability is described by the functions $\exp(\pm i\kappa_0 x)$, where κ_0 is defined by (17). The 'plus' sign is taken when $x > 0$ and the 'minus' sign is taken for $x < 0$. For a low-density beam, these functions are reduced to $\exp(\pm i k_z \sqrt{\varepsilon_0 u^2/c^2 - 1}\, x)$. These waves are therefore volume waves, as should be the case for propagating (emitted) waves (Fig. 3a). In the absence of instability (for $\varepsilon_0 = 1$), the beam wave is a surface wave (Fig. 3b). Figure 3 is plotted for the point $k_z = 5$ cm^{-1} of the dispersion curves in Fig. 2. The field decay for $|x| \to \infty$ shown in Fig. 3a is related to the delay in the transfer of perturbations and comes from the positive imaginary part of frequency.

If the vacuum channel is present in the dielectric, i.e., if $L \neq 0$, equation (18) is best studied numerically. Its approximate analytical solution can be easily obtained,[10] but is not presented here because it is unwieldy and uninformative. A numerical solution of equation (18) for a beam with the same parameters as in the case of Fig. 2 for several values of channel width L is shown in Fig. 4. For comparison, the complex correction to the frequency $\delta\omega$ for the case $L = 0$, taken from Fig. 2, is also shown.

It can be seen that, as L is increases, the growth rate decreases, which is particularly noticeable in the region of large wavenumbers k_z. The reason for this is that the field of the slow beam charge density wave decays as $\exp(-k_z\gamma^{-1}|x|)$ in the vacuum part of the system, where $|x| < L$ (Fig. 3b). So, the larger the product $k_z L$, the smaller the influence of the beam at the dielectric boundaries $x = \pm L$, where waves propagating to infinity are excited by the beam.

The maximum growth rate of dissipative–radiative instability is reached when the beam transport channel in the dielectric is absent. Furthermore, the growth rate increases infinitely as the wave number k_z increases, as can be seen from formula (25) and Fig. 2. It seems that this is an advantageous situation for MW electronics in terms of generating electromagnetic radiation of an arbitrary high frequency and in those frequency ranges where the generation of powerful radiation is associated with certain technical difficulties (e.g., in the terahertz range). However, this problem can only be considered solved on the basis of the results presented above if a material medium is found with a dielectric permittivity $\varepsilon_0 > c^2/u^2$ which is transparent to an

[8] This is the current through a cross section of area $A_b \times 1$ cm.

[9] The growth rate is only the imaginary part Im $\delta\omega$. The term 'complex increment' is used to denote the complex frequency correction $\delta\omega$.

[10] For that, we should replace the frequency ω by the Doppler frequency $k_z u$ in all terms of the equation except for the Cherenkov denominators.

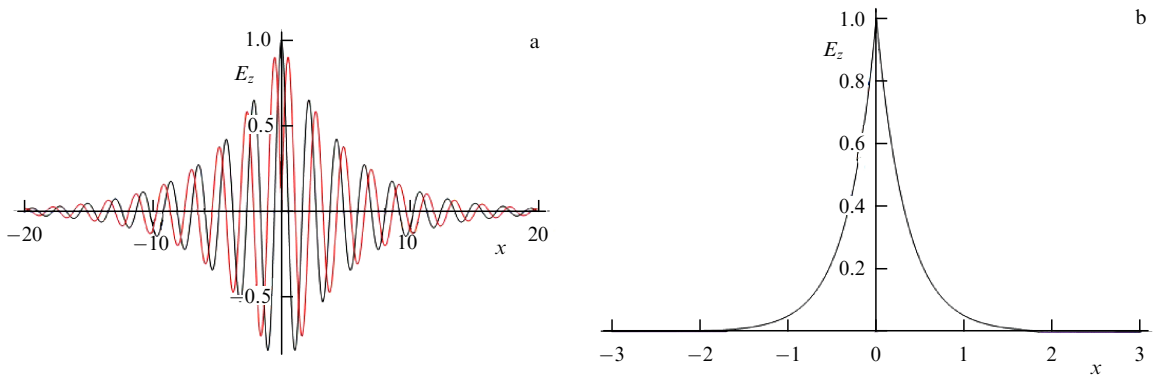

Figure 3. Beam wave field for (a) dissipative–radiative instability $\delta\omega = (-0.23 + 0.21i) \times 10^{10}$ rad s^{-1}, (b) slow wave $\delta\omega = -0.45 \times 10^{10}$ rad s^{-1}.

electric beam with a current of tens or hundreds of amperes. Otherwise, a channel must be provided for the beam to pass through the dielectric, and the electromagnetic field will necessarily decay transversely in this channel.[11]

4. Stimulated Cherenkov radiation and dissipative–radiative instability in layered system with isotropic plasma

We add complexity to the electrodynamic system we are considering by placing in the beam transport channel a cold collisionless isotropic plasma with the dielectric permittivity

$$\varepsilon_\perp = \varepsilon_\parallel = \varepsilon_\mathrm{p} = 1 - \frac{\omega_\mathrm{p}^2}{\omega^2}\,, \tag{26}$$

where ω_p is the Langmuir frequency of the plasma electrons.[12] In this case, $\chi_\perp^2 = k_z^2 - \varepsilon_\mathrm{p}\omega^2/c^2 = k_z^2 - \omega^2/c^2 + \omega_\mathrm{p}^2/c^2$, $\kappa = \chi_\perp$ in dispersion equation (18). Then, for $\omega_{\mathrm{b}0}^2 \Delta_\mathrm{b} = 0$, from equation (18), we obtain the following dispersion equation of the plasma Fabry–Pérot resonator:

$$\exp\left(-2\chi_\perp L\right) = \frac{\varepsilon_\mathrm{p}\chi_0^2 - \varepsilon_0\xi\chi_\perp}{\varepsilon_\mathrm{p}\chi_0^2 + \varepsilon_0\xi\chi_\perp}\,. \tag{27}$$

This equation defines a discrete set of eigenfrequencies like (20), with the only difference being that the frequencies are shifted upwards because of the plasma in the channel. The real parts of the frequencies are written as $\mathrm{Re}\,\omega \approx (\omega_\mathrm{p}^2 + k_z^2c^2 + k_{\perp n}^2c^2)^{1/2}$ instead of formula (20).

A cardinally new feature in the presence of plasma in the channel is the appearance of a surface wave caused by the interfaces between the plasma and the dielectric. The frequency of the surface wave is also defined by dispersion equation (27). Assuming that $\omega_\mathrm{p}c/L \gg 1$, we obtain from (27) a dispersion equation for the surface wave frequency spectrum $\varepsilon_\mathrm{p}\chi_0 + \varepsilon_0\chi_\perp = 0$, which leads to the following expression for the square of the frequency [4]:

$$\omega^2 = \frac{1}{2}\,\omega_\mathrm{p}^2 + \frac{\varepsilon_0+1}{2\varepsilon_0}\,k_z^2c^2 - \sqrt{\frac{1}{4}\,\omega_\mathrm{p}^4 + \left(\frac{\varepsilon_0+1}{2\varepsilon_0}\right)^2 k_z^4c^4 + \frac{\varepsilon_0-1}{2\varepsilon_0}\,\omega_\mathrm{p}^2k_z^2c^2}\,. \tag{28}$$

As the parameter $\omega_\mathrm{p}c/L$ decreases, the dependence $\omega(k_z)$ for the surface wave becomes flatter than (28). In any case, the phase velocity of the surface wave is always less than $c/\sqrt{\varepsilon_0}$. As this wave is not radiated, it is not attenuated.

In addition, for $\omega_{\mathrm{b}0}^2\Delta_\mathrm{b} = 0$, it follows from equation (18) that $\varepsilon_\mathrm{p} = 0$, which is the dispersion equation for longitudinal waves in isotropic plasma. The frequency of a longitudinal wave is $\omega = \omega_\mathrm{p}$, and the electric field component $E_z(x)$ can be an arbitrary function of the coordinate x, which is nonzero only within the plasma channel [18]; for $\varepsilon_\perp = \varepsilon_\parallel = \varepsilon_\mathrm{p} = 0$, this follows from equation (11).

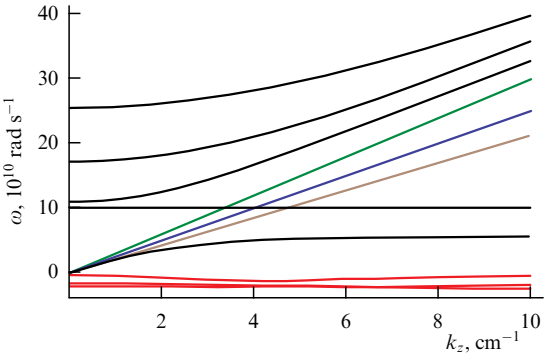

Figure 5. Eigenfrequencies of Fabry–Pérot resonator with a plasma channel: $\mathrm{Re}\,\omega$ (black), $\mathrm{Im}\,\omega$ (red), $\omega = k_zc$ (green), $\omega = k_zu$ (blue), and $\omega = k_zc/\sqrt{\varepsilon_0}$ (brown).

The general structure of the dispersion curves of an unbounded dielectric medium with a channel filled with isotropic plasma is shown in Fig. 5. The following parameters of the layered system are used: $L = 1$ cm, $\varepsilon_0 = 2$, $\omega_\mathrm{p} = 10^{11}$ rad s^{-1}. The curves are ordered in the upward direction as the dispersion curve of the surface wave, the straight line $\omega = \omega_\mathrm{p}$, and three dispersion curves of electromagnetic modes with $n = 0, 1, 2$. Also shown are the light line $\omega = k_zc$, the Cherenkov resonance line $\omega = k_zu$, and the light line of the dielectric $\omega = k_zc/\sqrt{\varepsilon_0}$. As can be seen from Fig. 5, for beam velocities in the range $u \in (c/\sqrt{\varepsilon_0}, c)$, where a dissipative–radiative instability is possible, there is also a Cherenkov resonance of the beam with the longitudinal plasma wave $\omega_\mathrm{p} = k_zu$. Cherenkov resonance with the surface wave is only possible for $u < c/\sqrt{\varepsilon_0}$, i.e., outside the region of dissipative–radiative instability.

In order to investigate the beam Cherenkov resonance with a Langmuir wave in a clean form, i.e., without any trace of dissipative–radiative instability, it is necessary to use the limit $L \to \infty$ or set $\varepsilon_0 = \varepsilon_\mathrm{p}$ in equation (18). As a result, we obtain the equation

$$1 - \frac{\omega_\mathrm{p}^2}{\omega^2} - \frac{1}{2}\,\Delta_\mathrm{b}\chi_\mathrm{p}\,\frac{\omega_{\mathrm{b}0}^2\gamma^{-3}}{(\omega - k_zu)^2} = 0\,, \quad \chi_\mathrm{p}^2 = k_z^2 - \frac{\varepsilon_\mathrm{p}\omega^2}{c^2}\,, \tag{29}$$

which describes the Cherenkov interaction of a thin ribbon magnetized beam with an unbounded isotropic electron plasma. Equation (29) has the form of equation (1) with $D_0(\omega, k_z) = 1 - \omega_\mathrm{p}^2/\omega^2$. If the coefficient $\Delta_\mathrm{b}\chi_\mathrm{p}/2$ in equation (29) is replaced by one, the result is the 'classical' dispersion equation, the analysis of which led to the discovery of beam instability in plasmas [20, 21]. However, this substitution is hardly legitimate. In fact, for the Cherenkov instability, $\omega \approx k_zu$; therefore, $\chi_\mathrm{p}^2 \approx \gamma^{-2}\omega^2/u^2 + \omega_\mathrm{p}^2/c^2$. Furthermore, since, for the instability at the plasma wave $\omega \approx \omega_\mathrm{p}$, then, for a relativistic beam, we get $\chi_\mathrm{p} \approx \omega_\mathrm{p}/c$. Equation (29) thus contains the parameter $\Delta_\mathrm{b}\omega_\mathrm{p}/c$, which is equal to the ratio of the beam thickness to the penetration depth of the transverse electromagnetic field in the plasma.

Under the inequality

$$\mu = \Delta_\mathrm{b}\,\frac{\omega_\mathrm{p}}{c}\,\frac{\omega_{\mathrm{b}0}^2\gamma^{-3}}{\omega_\mathrm{p}^2} \ll 1\,, \tag{30}$$

[11] A channeled electronic beam can be transported without loss in certain directions in crystalline dielectric media [17, 18]. However, the channeling effect can hardly be applied in electronics of even moderate power. Nevertheless, it can be claimed that one of the emission mechanisms from a channeled electron beam is based on a dissipative–radiative instability.

[12] The plasma can be considered nonmagnetized and the beam fully magnetized if the plasma density is large compared to that of the beam and the electron cyclotron frequency is small compared to the Langmuir frequency of the plasma electrons. Moreover, as mentioned in footnote 2, the requirement of magnetization is not necessary for a thin ribbon beam.

the solution of equation (29) has the form $\omega = k_z u + \delta\omega$, where

$$\delta\omega(k_z) = \begin{cases} \mathrm{i}k_z u\sqrt{\dfrac{\mu}{2}}, & k_z u \ll \omega_\mathrm{p}\,, \\ \dfrac{-1+\mathrm{i}\sqrt{3}}{2}\,\omega_\mathrm{p}\sqrt[3]{\dfrac{\mu}{2}}, & k_z u = \omega_\mathrm{p}\,. \end{cases} \tag{31}$$

The first expression in (31) gives the growth rate of nonresonant (aperiodic) beam instability due to the negativity of the plasma dielectric permittivity for $\omega \approx k_z u < \omega_\mathrm{p}$ (negative mass-type instability [5]), while the second defines the increment of the resonance instability for the stimulated Cherenkov effect. Note that dispersion equation (29) can be solved for a complex wave number k_z keeping a real frequency ω, which would define the wave amplification coefficient (spatial growth rate). In this case, the amplification coefficient will be infinite at the frequency $\omega = \omega_\mathrm{p}$. This is related to the independence of $D_0(\omega, k_z) = 1 - \omega_\mathrm{p}^2/\omega^2$ from the wave number. Infinity for the amplification coefficient can be easily eliminated, for example, by taking into account the spatial plasma dispersion caused by the thermal motion of electrons. If it is included, $D_0(\omega, k_z) = 1 - \omega_\mathrm{p}^2/(\omega^2 - k_z^2 V_\mathrm{Te}^2)$, where V_Te is a thermal electron velocity [6]. If $V_\mathrm{Te} \ll u$, then, when solving equation (29) for the frequency ω, the consideration of spatial dispersion is not important, as it leads to insignificant corrections.

Now consider the results of solving dispersion equation (18) for a finite width of the plasma channel. To reduce the number of free parameters, which increased by one due to the plasma compared to the previous case, we make use of dimensionless variables: the dimensionless frequency ω/ω_p and the dimensionless wave number $k_z c/\omega_\mathrm{p}$. The theory then depends on only one main parameter,

$$\sigma = \frac{L\omega_\mathrm{p}}{c}\,, \tag{32}$$

which is the ratio of the plasma half-width to the transverse field plasma penetration depth. One more parameter (30) does not play a significant role. We set it equal to 0.001. We also fix $\varepsilon_0 = 2$ and $u/c = 2.5/3$.

Figure 6 shows the dimensionless complex increments of the beam instability as a function of the dimensionless wave number for different values of parameter (32), i.e., for different plasma channel widths or plasma densities. The growth rates $\mathrm{Im}\,\omega$ show isolated sharp maxima at $k_z c/\omega_\mathrm{p} \approx 1.2$, which, as can be easily calculated, corresponds to the Cherenkov resonance point $k_z u/\omega_\mathrm{p} = 1$. These growth rate maxima are due to the stimulated Cherenkov effect at the Langmuir frequency $\omega = \omega_\mathrm{p}$. As parameter (32) is decreased, the instability increments related to the stimulated Cherenkov effect decrease, and for $\sigma = 0$ (the violet curve) they are not seen at all. In contrast, for $\sigma = 1$ (black curve), the instability growth rate due to the stimulated Cherenkov effect is maximal and hardly changes when the parameter σ is further increased. The case $\sigma = 1$ or greater corresponds to the instability described by dispersion equation (29) and formulas (31). However, in addition to the resonance instability on the Langmuir wave in the stimulated Cherenkov effect, the dependences shown in Fig. 6 describe another instability. Indeed, in the region $k_z u/\omega_\mathrm{p} > 1$, where no resonance Cherenkov instability can occur, there is an instability, and its increment is quite large. In the region $k_z u/\omega_\mathrm{p} > 1$, the increment is a smooth function of frequency, indicating that

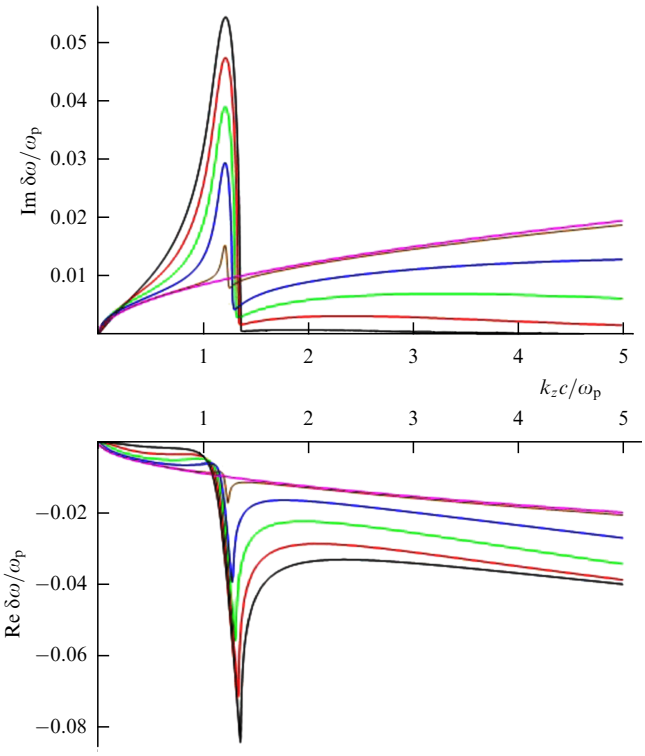

Figure 6. Complex increments of instability of electron beam in a homogeneous dielectric with a plasma channel: $\sigma = 1$ (black), 0.5 (red), 0.25 (green), 0.1 (blue), 0.01 (brown), and 0.0 (violet).

this instability is not resonant: it is the dissipative–radiative instability, or gain on radiation. For small values of parameter (32), the dissipative–radiative instability dominates, and for large values of this parameter, the stimulated Cherenkov effect dominates.[13]

The question arises as to why the role of dissipative–radiative instability decreases as parameter (32) is increased, and disappears completely as $\sigma \to \infty$. The point is that the wave number of the transverse wave in the plasma is $k_x = \sqrt{\varepsilon_\mathrm{p}\omega^2/c^2 - k_z^2}$. In this case, for $\omega \approx k_z u$, we have

$$k_x = \sqrt{\frac{\omega^2}{c^2} - k_z^2 - \frac{\omega_\mathrm{p}^2}{c^2}} \approx \mathrm{i}\sqrt{k_z^2\gamma^{-2} + \frac{\omega_\mathrm{p}^2}{c^2}}\,,$$

i.e., the wave decays with distance from the beam. Plasma screens the field of high-frequency beam density charge, and, the greater the plasma channel width L, the stronger the effect. This is why the dissipative–radiative instability ceases for $L \to \infty$, and for large but finite L its growth rate is proportional to $\exp(-\sigma)$, i.e., exponentially small. We note that, due to the thermal motion of electrons, another mechanism exists for the spatial decay of transverse waves in collisionless plasma — an anomalous skin effect [6]. The anomalous skin effect dominates in the low frequency range, when $|\omega| \ll kV_\mathrm{Te}$. In our case, $\omega \approx k_z u$ and $V_\mathrm{Te} \ll u$, and the anomalous skin effect plays no role.

It was mentioned earlier that the presence nonmagnetized plasma in the channel leads to the formation of a surface wave localized around the interface between the dielectric and plasma. As can be seen from formula (28), the phase velocity

[13] Weak indications of dissipative–radiative instability can be seen in Fig. 5 also for $\sigma = 1$, but already for $\sigma = 2$ they are absent from the plot.

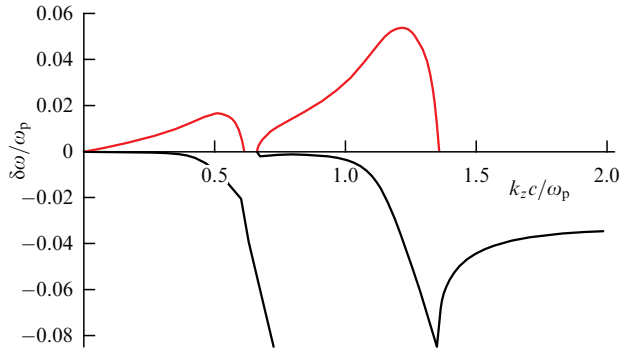

Figure 7. Complex increments of resonance Cherenkov instabilities for stimulated Cherenkov effect on a surface wave and on a volume Langmuir wave for $\sigma = 1$.

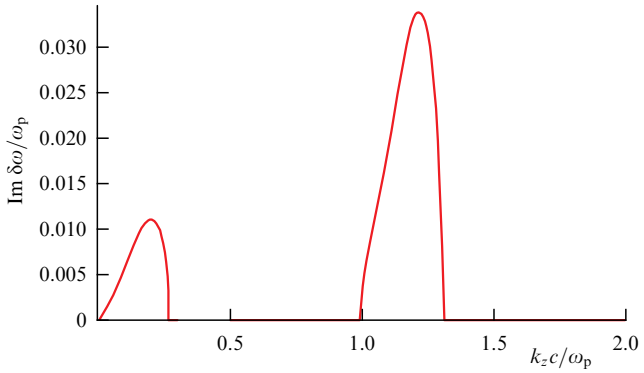

Figure 8. Growth rates of resonance Cherenkov instabilities on a surface wave and a volume Langmuir wave for $\sigma = 0.2$.

of this wave does not exceed $c/\sqrt{\varepsilon_0}$,[14] so it cannot be excited by a superluminal beam. To explore the excitation of a surface wave, consider the case of a subluminal beam $u < c/\sqrt{\varepsilon_0}$, when the dissipative–radiative instability is absent, but the resonant Cherenkov excitation of both the surface wave and the volume Langmuir wave is possible. To keep the beam parameters unchanged, we set $\varepsilon_0 = 1$ when solving dispersion equation (18). The result for the case $\sigma = 1$ is shown in Fig. 7.

There are two intervals of wavenumbers where the imaginary frequency part is positive, i.e., there is a beam instability (red lines). The left interval is related to the instability on the surface wave, and the right interval, to the instability on the volume Langmuir wave. It is noteworthy that two different independent solutions of dispersion equation (18) are responsible for these instabilities. Indeed, no connection between these solutions can be seen in Fig. 7 (there are two nonintersecting complex curves $\delta\omega(k_z)$). In contrast, for the stimulated Cherenkov effect on the volume Langmuir wave and dissipative–radiative instability, there is a single solution (Fig. 6 shows a single continuous curve $\delta\omega(k_z)$) describing one instability or the other in different frequency intervals.

Figure 8 shows dimensionless increments for the same instabilities as in Fig. 7, but for the case $\sigma = 0.2$. It can be seen that the instability interval on the surface wave becomes narrower and is shifted to the left, while the increment becomes smaller. The explanation is that, as the parameter σ decreases, the surface wave frequency also decreases, and the surface wave disappears altogether for $\sigma \to 0$. The narrowing of the instability interval and the decrease in its growth rate are also observed for the instability on the volume Langmuir wave. It should be noted that, in this case, unlike in formula (31) and the case shown in Fig. 6, the lower limit of the instability interval is not zero and becomes higher as the parameter σ grows. This is because the region of nonresonant (aperiodic) instability disappears, which is caused by the change of the sign of the effective dielectric permittivity of the layered system in the low-frequency range.

[14] Formula (28) is obtained in the limit $\sigma \to \infty$. For a finite σ, the surface wave dispersion curve passes below the curve defined by (28).

5. Stimulated Cherenkov radiation and gain on radiation in layered system with strongly anisotropic plasma

Let us also consider the case where the plasma in the channel is fully magnetized. This case is of considerable practical interest, since most of the powerful sources of electromagnetic radiation created to date in plasma MW electronics operate on plasma waves in a strong external magnetic field [22–24]. As will be seen below, the cases of nonmagnetized plasma (see Section 4) and fully magnetized plasma are cardinally different. An intermediate case — plasma in a finite external magnetic field — is rather complicated in the context of our problem, and its consideration is beyond the scope of the present work. It is generally assumed that, for $\Omega_e < \omega_p$, where Ω_e is the electron cyclotron frequency, a plasma can be regarded as nonmagnetized in the frequency range $\Omega_e < \omega < \omega_p$. Conversely, for $\Omega_e > \omega_p$, the plasma can be considered fully magnetized in the first approximation. In the case of fully magnetized plasma $\varepsilon_\perp = 1$, $\varepsilon_\parallel = \varepsilon_p$, and ε_p is defined in (26). In this case, we have $\chi_\perp^2 = k_z^2 - \omega^2/c^2$, $\kappa = (\chi_\perp^2 \varepsilon_p)^{1/2}$ in equation (18). For $\omega_{b0}^2 \Delta_b = 0$, the following equation for the eigenfrequencies of the Fabry–Pérot resonator formed by a layer of fully magnetized plasma is obtained from (18):

$$\exp\left(-2\sqrt{\chi_\perp^2 \varepsilon_p}\, L\right) = \frac{\chi_0^2 \sqrt{\chi_\perp^2 \varepsilon_p} - \varepsilon_0 \xi \chi_\perp^2}{\chi_0^2 \sqrt{\chi_\perp^2 \varepsilon_p} + \varepsilon_0 \xi \chi_\perp^2}\,. \tag{33}$$

Equation (33) has solutions only in the range of frequencies and wavenumbers defined by the inequality

$$-\chi_\perp^2 \varepsilon_p = -\left(k_z^2 - \frac{\omega^2}{c^2}\right)\left(1 - \frac{\omega_p^2}{\omega^2}\right) \equiv k_x^2 > 0\,. \tag{34}$$

Inequality (34) is satisfied in two ranges of frequencies and wavenumbers. The first range,

$$\omega > \max\left(\omega_p, k_z c\right), \tag{35}$$

includes solutions of equation (33) which are similar to the solutions shown for the region (35) in Fig. 5. We are not interested in such solutions, since they describe waves with phase velocities exceeding the speed of light in a vacuum. The second range,

$$\omega < \min\left(\omega_p, k_z c\right), \tag{36}$$

includes solutions describing so-called oblique Langmuir waves [3, 25]. The quantity k_x introduced in (34) is the

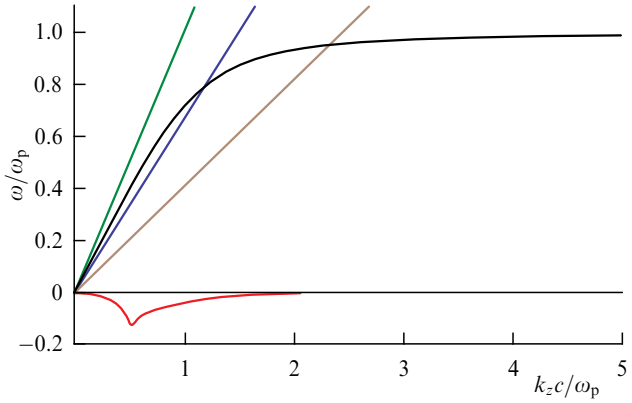

Figure 9. Main mode of oblique Langmuir wave: real frequency part (black) and imaginary part (red).

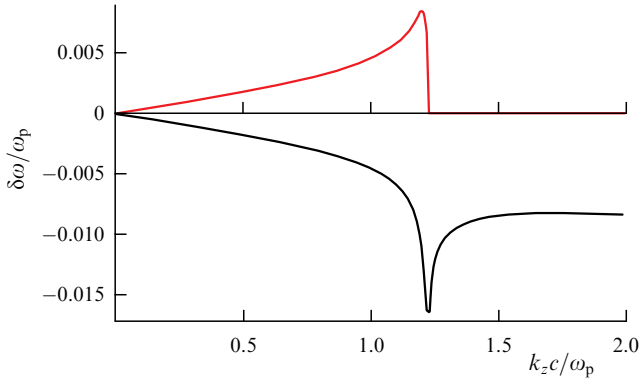

Figure 10. Complex argument of Cherenkov instability of a thin ribbon electron beam in fully magnetized unbounded plasma.

transverse wavenumber of the eigenwave of the Fabry–Pérot resonator. This number is defined by the plasma layer thickness. The formula

$$k_x = k_{\perp n} = \frac{\pi}{L}(n + a_n), \quad n = 0, 1, 2, \ldots \tag{37}$$

is valid, where the quantities a_n are slightly different from 1/2 (see (20)). The complex dispersion curve of the main mode (with $n = 0$) of the oblique Langmuir wave is plotted in Fig. 9. The imaginary frequency part (red curve) is shown scaled up by a factor of 10. All other features of Fig. 9 are the same as in Fig. 5. The dispersion curves of the higher modes (with $n \geqslant 1$) of an oblique Langmuir wave (not shown in the figure) pass below the dispersion curve of the main mode.

The field structure of oblique Langmuir waves is described by the oscillating functions $\exp(\pm \mathrm{i} k_x x)$, as can be seen from (34) and formula (15), which corresponds to a volume wave in the plasma layer. The limit transition $L \to \infty$ in equation (18) is not obvious due to the oscillating behavior of the exponential factor $\exp(-2\kappa L)$. However, assuming that the imaginary part of ω is positive, the factor $\exp(-2\kappa L)$ will tend to zero as $L \to \infty$. As for the assumption that the imaginary part of the frequency is positive, in a general case it is due to the causality principle, and, in our case, it is related to the beam instability. Thus, taking the limit $L \to \infty$, equation (18) reduces to the following dispersion:

$$\sqrt{1 - \frac{\omega_p^2}{\omega^2}} - \frac{1}{2}\,\Delta_b \sqrt{k_z^2 - \frac{\omega^2}{c^2}}\,\frac{\omega_{b0}^2 \gamma^{-3}}{(\omega - k_z u)^2} = 0\,, \tag{38}$$

which describes the Cherenkov interaction of a thin ribbon electron beam with a fully magnetized unbounded plasma for a beam moving along an external magnetic field. Equation (38) can be obtained directly, without taking the limit, by inserting $E_z(x) = A \exp(\mathrm{i} k_x x)$ into boundary condition (12), with account for (14), where the wave number k_x is defined in (34).

Although equation (38) does not have a common form (the square root dependence on the plasma dielectric permittivity), it is solved in the usual way. The solution is sought in the form $\omega = k_z u + \delta\omega$, where $|\delta\omega| \ll k_z u$. After simple calculations the complex increments are written as

$$\delta\omega = \frac{-1 + \mathrm{i}}{\sqrt{2}} \left(\frac{1}{2}\,\Delta_b k_z \omega_b^2 \gamma^{-4} \frac{k_z u}{\omega_p}\right)^{1/2}, \quad k_z u \ll \omega_p\,, \tag{39a}$$

$$\delta\omega = \exp\left(\frac{\mathrm{i}4\pi}{5}\right) \left(\frac{1}{2}\,\Delta_b k_z \omega_b^2 \gamma^{-4} \sqrt{\frac{\omega_p}{2}}\right)^{2/5}, \quad k_z u = \omega_p\,^{15}. \tag{39b}$$

The result of numerically solving equation (38) for $\mu = 0.0001$ and $u/c = 2.5/3$ is shown in Fig. 10. There is good agreement with analytical formulas (39).

Let us try to classify the instability described by dispersion equation (38). For $L \to \infty$, the quantity k_x in (34) is the wave number of an oblique Langmuir wave propagating to infinity, and from (37) it follows that the wave number k_x can be arbitrary (even though $L^{-1} \to 0$, the number n can be arbitrarily high). Inserting $\omega = k_z u$ into (34) gives

$$k_x = k_z \gamma^{-1} \sqrt{\frac{\omega_p^2}{k_z^2 u^2} - 1}\,. \tag{40}$$

From (40), it follows that the emission to infinity through a plasma half-space is only possible for $k_z u \approx \omega < \omega_p$. Therefore, if $k_z u > \omega_p$, the instability increment in Fig. 10 becomes zero. Formula (40) allows the instability mechanism to be linked to the emission to infinity of oblique plasma waves excited by the beam, i.e., to attribute the instability to a dissipative–radiative one. This conclusion is also consistent with the structure of dispersive equation (38) and with the fact that, in semi-bounded plasma, the wave (34) is not an eigenwave. This is different from the case of isotropic plasma. In this case, the instability with the second increment (31) was clearly related to the stimulated Cherenkov effect. The point is that this instability develops on the longitudinal Langmuir wave $\omega = \omega_p$. Such a wave, unlike the oblique Langmuir wave of a plasma half-space in a strong magnetic field, is an eigenwave, and, in addition, it is not radiated (the longitudinal wave of cold plasmas does not transfer any energy at all, since it has a zero group velocity).

As in the case of isotropic plasma, for fully magnetized plasma, there is no beam instability for $L \to \infty$ in the wave number range defined by the inequality $k_z u > \omega_p$ (see Fig. 10 and the black curve in Fig. 6); electromagnetic waves with phase velocities smaller than the light speed c are absent in these plasmas in the region $\omega > \omega_p$. The dielectric medium, where, for $u > c/\sqrt{\varepsilon_0}$, there are waves with phase velocities close to u, are too far away from the beam for $L \to \infty$. The situation is completely different when the plasma channel has

[15] $\exp(\mathrm{i}4\pi/5) \approx -0.81 + 0.59\mathrm{i}$.

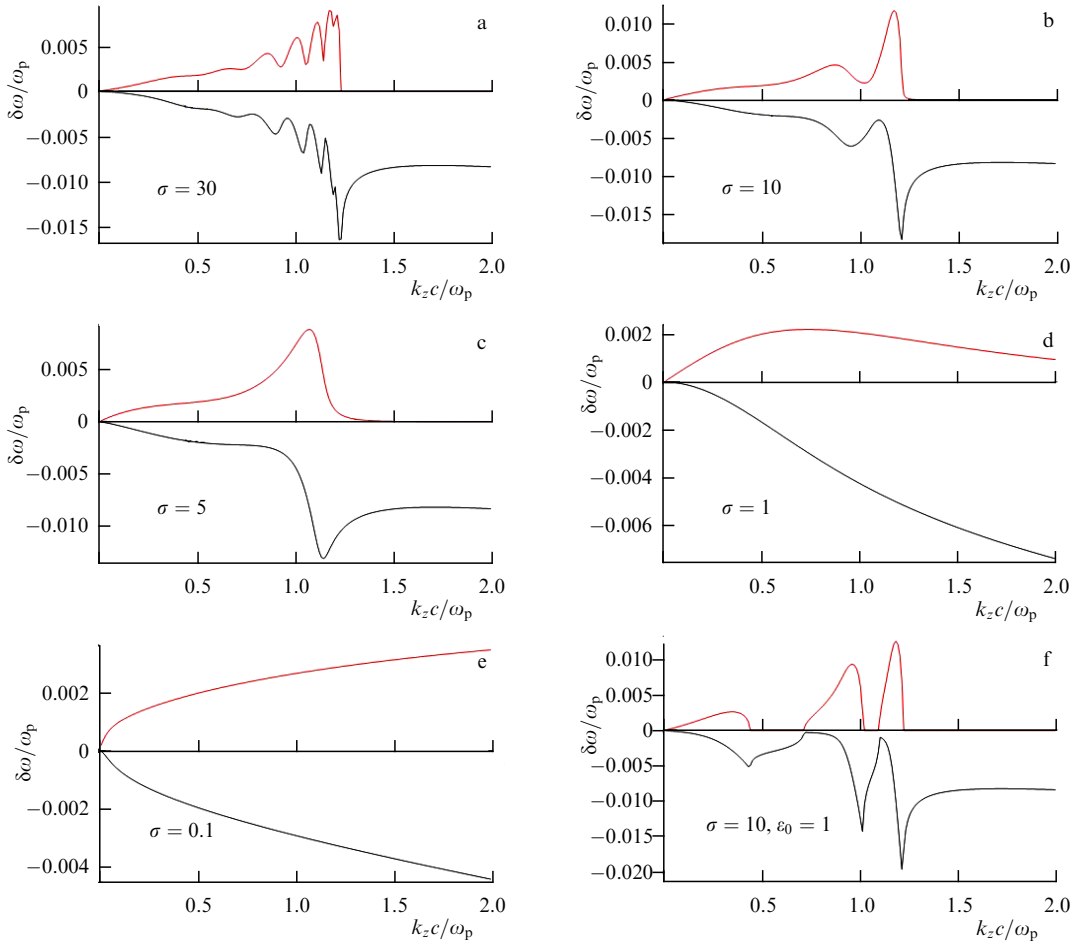

Figure 11. Increments of beam instability in dielectric system with layer of magnetized plasma.

a finite width L. In this case, radiating electromagnetic waves are excited in the dielectric, transferring the beam energy to infinity. The result is a dissipative–radiative instability in the range $k_z u > \omega_p$.

For a finite L, the resonance properties of the layered system come into play: quasi-standing waves with wavenumbers (37) are formed in the plasma layer, i.e., the eigenmodes of the Fabry–Pérot resonator manifest themselves. The eigenmodes formed by oblique Langmuir waves can be in the Cherenkov resonance with the beam.[16] Inserting the transverse wavenumbers (37) and the longitudinal wavenumber $k_z = \omega/u$ into (34), we obtain for the resonant frequencies

$$\omega = \sqrt{\omega_p^2 - k_{\perp n}^2 u^2 \gamma^2}\,. \tag{41}$$

The instability of the stimulated Cherenkov effect should manifest itself at these frequencies: it will be superimposed in some way on the dissipative–radiative instability. For a decreasing channel width L, the numbers $k_{\perp n}$ increase and the number of resonances (41) decreases, and starting from some L resonances disappear completely. In this case, the instability in the stimulated Cherenkov effect disappears, and only the dissipative–radiative instability remains.

Figure 11 shows complex increments of instabilities accompanying a ribbon beam in a channel with a fully magnetized plasma for different values of the parameter σ, obtained by numerically solving equation (18). To make the resonance effects more apparent, the calculations have taken parameter (30) to be an order of magnitude smaller than when solving equation (18) in the case of isotropic plasma in the channel, $\mu = 0.0001$. For $\sigma = 30$ (Fig. 11a), five local extrema of the increment stand out quite clearly. These maxima are associated with the stimulated Cherenkov effect for several modes of an oblique Langmuir wave with numbers from zero to 4 or 5. The number of maxima increases as σ increases. They merge for $\sigma = \infty$, leading to the complex increment behavior shown in Fig. 10. As σ is reduced, the number of resonance maxima decreases: there are two maxima in Fig. 11b and only one in Fig. 11c. For even smaller values of the parameter σ, the resonance maxima of the increment disappear (Fig. 11d, e).

In the cases $\sigma = 1$ and $\sigma = 0.1$ (Fig. 11d, e), the instability is only of a dissipative–radiative nature. The dependences plotted in Fig. 11e have the same form as the corresponding ones in Fig. 2 (differences in values are due to different μ used in the calculations). In other cases (Fig. 11a–c), we are dealing with two instabilities simultaneously: the dissipative–radiative one and the one in the stimulated Cherenkov effect. Their contribution to the net increment depends on the wave number k_z. To be sure that two instabilities coexist, a special calculation was carried out for the same system, but under conditions where one of the instabilities is absent. We took $\varepsilon_0 = 1$. In this case, a dissipative–radiative instability cannot evolve, but the instability of the stimulated Cherenkov effect

[16] These waves are standing in the x direction and travel in the z direction.

remains in its present form. The result is shown in Fig. 11e. We identify the same resonance maxima as in Fig. 11b, but the increment is zero in the intervals between them, which is due to the absence of the contribution from the dissipative–radiative instability. In general, the smaller the parameter σ (32), the greater the role of the dissipative–radiative instability. This should be clear — the smaller σ, the smaller the distance L from the beam to the dielectric.

There is another instability that is, in principle, possible in a system with a layer of fully magnetized plasma — this is a resonance instability with the stimulated Cherenkov effect in a dissipative system, when the dissipation is caused by radiation. As can be seen from Fig. 9, in the wavenumber range where there is Cherenkov resonance of the electron beam with an oblique Langmuir wave, this wave decays as it is radiated through the layer boundaries at $x = \pm L$. Thus, the stimulated Cherenkov effect turns out to be possible on the decaying eigenwave of the electrodynamic system. We present here the necessary information about such an instability based on the general dispersion equation (1) [13].

If the dispersion function is complex, $D_0 = D_0' + \mathrm{i}D_0''$, and the condition of the Cherenkov resonance holds $D_0'(k_z u, k_z) = 0$, then, by writing $\omega = \omega_0 + \delta\omega$ and $k_z = k_{z0}$, it is not difficult to obtain from dispersion equation (1) the following equation for the complex increment $\delta\omega$:

$$\delta\omega^2 \left(\mathrm{i}D_0'' + \delta\omega \frac{\partial D_0'}{\partial \omega} \right) - \alpha\omega_\mathrm{b}^2 = 0 \,. \tag{42}$$

If the inequality

$$|D_0''| \ll \left| \delta\omega \frac{\partial D_0'}{\partial \omega} \right| \tag{43}$$

is observed, equation (42) leads to expression (3) (after replacing D_0 by D_0'), which defines the increment of the usual instability in the stimulated Cherenkov effect. If the inequality is reversed, equation (42) gives

$$\delta\omega = \pm \sqrt{\frac{\mathrm{i}\alpha\omega_\mathrm{b}^2}{D_0''}} \,. \tag{44}$$

Quantity (44) with the positive imaginary part is the increment of the resonance instability when there is a stimulated Cherenkov effect in a dissipative system. The condition for this effect to exist is the inequality opposite to (43), which, taking into account (44), can be reduced to

$$|D_0''|^3 \gg \alpha\omega_\mathrm{b}^2 \left(\frac{\partial D_0'}{\partial \omega} \right)^2 . \tag{45}$$

The question arises as to whether it is this instability that is realized at the maxima of the increment in Fig. 11a. A direct verification of inequality (45) is difficult due to the complexity of the left-hand side of equation (18). There are indirect considerations based on the fact that the decay rate of the oblique Langmuir wave is very small. In Fig. 9, this decay rate (red line) is plotted amplified 10 times, as it would be practically impossible to show it graphically otherwise. It is very likely that, in the cases we have considered, a usual stimulated Cherenkov effect takes place, and not a dissipative one.

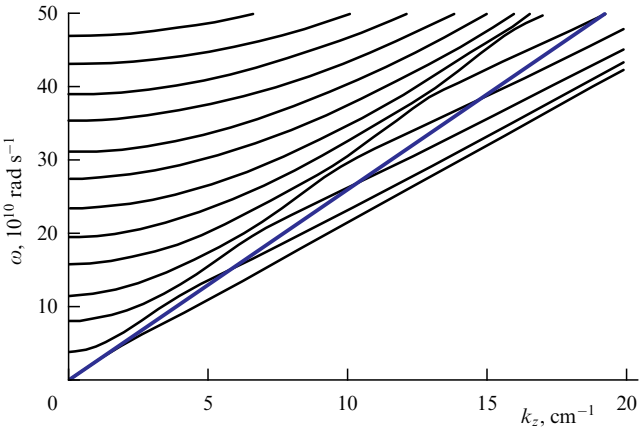

Figure 12. Dispersion curves of dielectric waveguide with a vacuum channel; line of Cherenkov resonance $\omega = k_z u$, $u/c = 2.5/3$ (blue).

6. Transition from waveguide to unbounded system

We place the system under consideration in a plane waveguide formed by two ideally conducting planes $x = \pm L_\infty$, where $L_\infty > L$. The derivation of the dispersion equation for the eigenmodes of such a waveguide is carried out in the same way as the derivation of equation (18), with the only difference being that solution (16) should be replaced by the solution

$$E_z = C \sinh\left[\xi(L_\infty - x)\right], \quad L < x < L_\infty \,. \tag{46}$$

Here, we took into account that the field component E_z is zero at ideally conducting waveguide walls. After standard manipulations, we find

$$\frac{(\varepsilon_\perp \kappa\chi_0^2 - \varepsilon_0 \xi \chi_\perp^2 G) - (\varepsilon_\perp \kappa\chi_0^2 + \varepsilon_0 \xi \chi_\perp^2 G) \exp(-2\kappa L)}{(\varepsilon_\perp \kappa\chi_0^2 - \varepsilon_0 \xi \chi_\perp^2 G) + (\varepsilon_\perp \kappa\chi_0^2 + \varepsilon_0 \xi \chi_\perp^2 G) \exp(-2\kappa L)} = \frac{1}{2} \Delta_\mathrm{b} \frac{\chi_\perp^2}{\kappa\varepsilon_\perp} \frac{\omega_{\mathrm{b}0}^2 \gamma^{-3}}{(\omega - k_z u)^2} \,, \tag{47}$$

where

$$G = -\coth\left[\xi(L_\infty - L)\right] . \tag{48}$$

It can be easily shown that, in the limit $L_\infty \to \infty$, quantity (48) tends to one and equation (47) transforms into equation (18). Note that, when taking this limit, in accordance with the causality principle, it is necessary to assume that the frequency ω has a positive imaginary part. Then, the equation obtained in the limit should be analytically continued in the lower half-plane of the complex plane ω to obtain a full equivalent of equation (18).

There is a fundamental difference between equations (47) and (18): the zeros on the left-hand side of equation (47) define real frequencies of nondecaying eigenmodes in the waveguide, while those on the left-hand side of equation (18) define complex frequencies of the decaying eigenmodes of the Fabry–Pérot resonator. We illustrate this with an example. Figure 12 shows the dispersion curves of the eigenmodes of the dielectric waveguide containing a vacuum channel. The waveguide parameters are $L_\infty = 2$ cm, $L = 1$ cm, $\varepsilon_0 = 2$. A large number of dispersion curves of the waveguide eigen-

modes can be seen, starting with the TEM mode (lowest curve) and ending with the mode E_n with $n = 11$. In the short-wave region, the phase velocities of all these modes approach $c/\sqrt{\varepsilon_0}$ and, therefore, if the beam is superluminal, it can be in the Cherenkov resonance with all the eigenmodes of the waveguide. The complex frequencies of the eigenmodes of the Fabry–Pérot resonator, formed by a flat vacuum channel in the dielectric, are given by formulas (20). Obviously, Cherenkov resonance of a beam with such waves is impossible.

The difference between equations (47) and (18) is particularly noticeable at $L = 0$, i.e., in the absence of the beam transport channel in the dielectric. In this case, the resonator is eliminated, while the waveguide and its eigenmodes are available. Substituting $L = 0$ (or $\varepsilon_\perp = \varepsilon_\parallel = \varepsilon_0$) into equation (47) gives a dispersion equation which defines the complex frequencies of a homogeneous dielectric waveguide with a thin ribbon electron beam,

$$\xi \cosh(\xi L_\infty) = \sinh(\xi L_\infty)\chi_0^2 \frac{1}{2} \Delta_b \frac{\omega_{b0}^2 \gamma^{-3}}{\varepsilon_0(\omega - k_z u)^2} . \quad (49)$$

Equation (49) has the form of the general dispersion equation (1). The zeros on its left-hand side, i.e., the roots of the equation $\xi \cosh(\xi L_\infty) = i\kappa_0 \cos(\kappa_0 L_\infty) = 0$, define the frequencies of the eigenwaves of the waveguide without a beam,

$$\omega = \sqrt{k_{\perp n}^2 + k_z^2}\, \frac{c}{\sqrt{\varepsilon_0}} , \quad k_{\perp n} = \frac{\pi}{L_\infty}\left(n + \frac{1}{2}\right), \quad n = 0, 1, \ldots . \quad (50)$$

One more root, $\kappa_0 = 0 \to \omega = k_z c/\sqrt{\varepsilon_0}$, sets the frequency of the TEM wave, which is of no interest to us here.[17] Inserting $k_z = \omega/u$ into (50), we find an infinite set of resonance frequencies

$$\omega_n = \frac{k_{\perp n} u}{\sqrt{\varepsilon_0 u^2/c^2 - 1}} . \quad (51)$$

Inserting further $\omega = \omega_n + \delta\omega$, $k_z = k_{zn} = \omega_n/u$ into equation (49), we find the following increments of instabilities on eigenmodes of the dielectric waveguide in the stimulated Cherenkov effect:

$$\delta\omega = \delta\omega_n = \frac{-1 + i\sqrt{3}}{2}\left(\frac{\Delta_b}{2L_\infty}\frac{k_{\perp n}^2 c^2}{\varepsilon_0 \omega_n}\frac{\omega_b^2 \gamma^{-3}}{\varepsilon_0}\right)^{1/3} . \quad (52)$$

In the limit $L_\infty \to \infty$, equation (49) reduces to

$$\xi = -\chi_0^2 \frac{1}{2} \Delta_b \frac{\omega_{b0}^2 \gamma^{-3}}{\varepsilon_0(\omega - k_z u)^2} . \quad (53)$$

The zero on the left-hand side of equation (53) defines a light wave $\xi = 0 \to \omega = k_z c/\sqrt{\varepsilon_0}$, propagating strictly along the beam propagation direction, with which the beam does not interact. There are no other eigenwaves, since the resonator is absent for $L = 0$, and the dielectric half-spaces $x > 0$ and $x < 0$, so to speak, do not 'hold' the wave.[18] Taking into account that, according to (16) and (17), $\xi = i\kappa_0$, $\chi_0^2 = -\kappa_0^2$, we transform equation (53) into equation (23), which we studied in detail earlier. The solution to equation (23) is given in (25).

Thus, the differences between equations (49) and (53), as well as between their solutions (52) and (25), are obvious. This also applies to the most general equations (18) and (47). In the limit $L_\infty \to \infty$, solutions of equation (47) describing instability should transform into corresponding solutions of equation (18). For example, quantities (52) $\delta\omega_n = \delta\omega(k_{zn})$ for $L_\infty \to \infty$ should transform into the function $\delta\omega(k_z)$, which is defined by the second term on the right-hand side of expression (25) (at common points $k_z = k_{zn}$). To illustrate the 'dynamics' of this limit transition, let us consider numerical solutions of equation (49) for different values of the parameter L_∞, with other parameters fixed at the values used in the calculations for Fig. 2. Figure 13a shows a sequence of isolated local maxima of the imaginary part of the complex increment $\delta\omega$ (red line). The maxima are located at the resonance points $k_z = k_{zn}$ and agree reasonably well with formula (52). Each maximum and its vicinity describe an instability of the stimulated Cherenkov effect on the mode E_n of the dielectric waveguide. As L_∞ is increased (Fig. 13b, c), the local maxima appear closer to each other and begin to merge, the effect becoming stronger as k_z increases. Finally, for $L_\infty = 40$ cm (Fig. 13d), the increment maxima disappear completely and a smooth dependence is formed, which is well described by the second term on the right-hand side of formula (25). The curves shown in Fig. 13d coincide with the respective curves in Fig. 2 obtained by numerically solving equation (23). This behavior is due, first and foremost, to the fact that, as L_∞ increases, the resonance wavenumbers $k_{zn} = \omega_n/u$ become denser, and for $L_\infty \to \infty$ fill the entire axis $k_z > 0$.

For any finite value of parameter L_∞, the beam resonantly excites the eigenwaves in the waveguide. The instabilities that arise in this case clearly correspond to our definition for the instability of the stimulated Cherenkov effect. Therefore, taking into account the limit transition $L_\infty \to \infty$ described above, the question arises as to the relevance of the notion of dissipative–radiative instability introduced above. Admittedly, for the large parameter L_∞, the expressions for the increments vary considerably, first and foremost because of the closer position of the eigenwaves of the electrodynamic system. In MW electronics, electrodynamic systems with a close arrangement of eigenmodes are called spatially developed systems. The interaction of electron beams with densely arranged eigenmodes of spatially developed electrodynamic systems has been studied in detail [26, 27]. Therefore, instead of dissipative–radiative instability, it is fully legitimate to talk about an instability of the stimulated Cherenkov effect in a spatially developed electrodynamic system. A criterion for such an instability is the inequality $|\delta\omega| \gg \omega_{n+1} - \omega_n$, where $\delta\omega$ is the instability increment. Taking into account formulas (50) and (51), we write this inequality as

$$|\delta\omega| \gg \frac{u}{L_\infty}\frac{\pi}{\sqrt{\varepsilon_0 u^2/c^2 - 1}} , \quad (54)$$

where $\delta\omega$ is the increment (52). If inequality (54) holds, the instability increment is defined by formula (25) instead of (52).

However, based on physical considerations, the term dissipative–radiative instability seems to us to be perfectly

[17] For a TEM wave, the electric field component in the direction of the beam motion equals zero. Therefore, a TEM wave cannot be excited by a straight beam, as can be seen from equation (49), whose right-hand side becomes zero for $\xi = 0$.

[18] In the half-spaces, there are eigenwaves coming from infinity of one sign and propagating to infinity of the other sign. Our problem statement excludes waves coming from infinity.

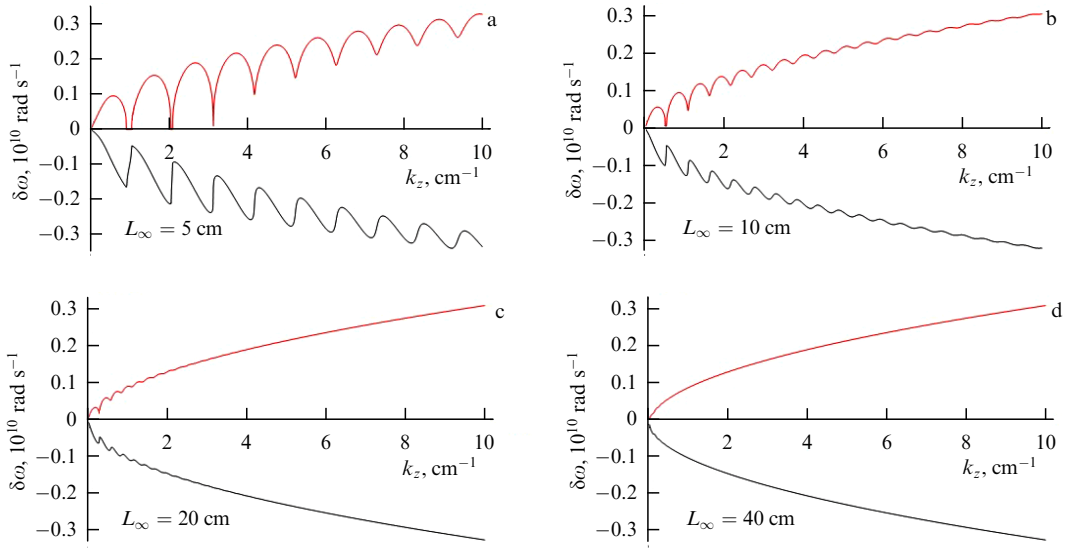

Figure 13. Instability increments of stimulated Cherenkov effect on eigenmodes of homogeneous dielectric waveguide.

rational: for an eigenmode to be established, it takes a time not shorter than

$$\tau_0 = \frac{2\sqrt{\varepsilon_0}\,L_\infty}{c}\,. \tag{55}$$

On the other hand, the characteristic time of instability development τ_b (from the onset to its nonlinear saturation) is defined by the instability increment, commonly as $\tau_\mathrm{b} \sim \delta\omega^{-1}$ [28]. For $\tau_\mathrm{b} < \tau_0$, an eigenmode has no time to settle in the system during the instability development interval, and the electron beam excites waves that propagate from the beam to the outer waveguide boundaries but do not reach them. In the case of the initial value problem, solved from the moment of 'switching on' of the instability to its saturation, everything happens namely so. The strong inequality $\tau_\mathrm{b} < \tau_0$ is reduced to

$$|\delta\omega| \gg \frac{c}{L_\infty}\frac{1}{2\sqrt{\varepsilon_0}}\,, \tag{56}$$

which does not contradict (54). Indeed, if inequality (56) is observed, there is reason to speak of dissipative–radiative instability.

The dissipative–radiative instability is a nonresonance instability. This means that there is no resonance wave with which the beam can interact. The beam interacts with the waves of the continuous spectrum $\omega \approx k_z c/\sqrt{\varepsilon_0}$, i.e., with many waves of different frequencies. It is impossible to capture the beam electrons under these conditions. Instead, the beam electrons decelerate to a velocity approaching $c/\sqrt{\varepsilon_0}$. From these considerations, it is easy to estimate the fraction of the beam kinetic energy transferred to electromagnetic radiation,

$$\eta = \frac{\gamma_\infty - \gamma}{\gamma - 1} = \frac{\gamma}{\gamma - 1}\left[1 - \left(1 + 2\gamma^2\,\frac{u^2}{c^2}\left(1 - \frac{c}{u\sqrt{\varepsilon_0}}\right)\right)^{-1/2}\right], \tag{57}$$

where γ_∞ is the relativistic factor of beam electrons on the instability saturation stage. Dependence (57) is plotted in Fig. 14 for three values of the dielectric permittivity ε_0.

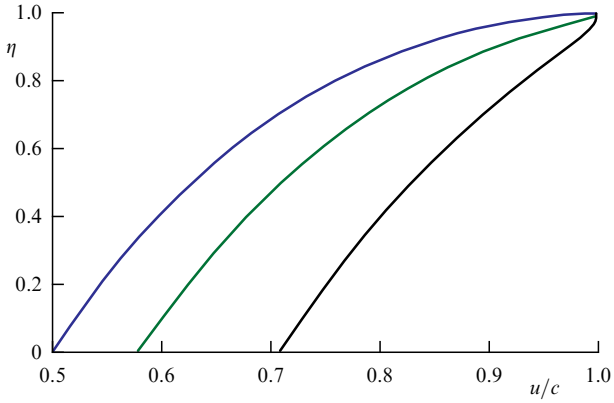

Figure 14. Share of beam energy transferred to radiation in dissipative–radiative instability: $\varepsilon_0 = 2, 3, 4$ from right to left.

7. Dissipative–radiative instabilities in cylindrical geometry

In a cylindrical coordinate system for an azimuthally symmetric case, equation (11) takes the form

$$\frac{1}{r}\frac{\mathrm{d}}{\mathrm{d}r}\left(r\,\frac{\varepsilon_{rr}(r)}{\chi_{rr}^2(r)}\,\frac{\mathrm{d}E_z}{\mathrm{d}r}\right) = \left[\varepsilon_{zz}(r) + \delta\varepsilon_\mathrm{b}(r)\right]E_z\,, \tag{58}$$

while formulas (10) stay valid after an obvious replacement of $|x|$ by r and L by R, where R is the radius of the beam transport channel. To avoid the difficulties caused by the singular point $r = 0$, we consider an infinitely thin tubular beam with the Langmuir frequency given by the formula

$$\omega_\mathrm{b}^2(r) = \omega_{\mathrm{b}0}^2 \Delta_\mathrm{b}\delta(r - r_\mathrm{b})\,, \tag{59}$$

where $r_\mathrm{b} \neq 0$ is the radius of the tubular beam. Integrating equation (58) over r, we obtain the following condition for the jump of the derivative of $E_z(r)$ on the beam:

$$\left\{\frac{\mathrm{d}E_z}{\mathrm{d}r}\right\}_{r=r_\mathrm{b}} = -\Delta_\mathrm{b}\chi_\perp^2\,\frac{\omega_{\mathrm{b}0}^2\gamma^{-3}}{\varepsilon_\perp(\omega - k_z u)^2}\,E_z(r_\mathrm{b})\,, \tag{60}$$

$$\chi_\perp^2 = k_z^2 - \frac{\omega^2}{c^2}\,\varepsilon_\perp\,.$$

Boundary conditions (13) continue to hold with the above substitutions, and, instead of condition (14), a condition is written that the field is bounded at zero, $E_z(0) < \infty$. Note that a cylindrical system with radiation exiting through the side surface or with an outer absorbing layer (Fig. 1b) is of considerable practical interest. Recent active studies are aimed at the design of broadband plasma MW amplifiers based on tubular relativistic electron beams with electromagnetic wave absorbers on the side surface of the plasma electrodynamic system [24]. The absorber is intended to suppress the self-excitation of the amplifier by absorbing a feedback wave. However, the presence of the absorber facilitates the development of a nonresonant dissipative–radiative instability, which requires the study of this instability in new devices of MW plasma electronics.

We will not solve the general problem formulated for the spherical geometry here, but restrict ourselves to the limit $R = 0$. Consider two cases: $\varepsilon_\perp = \varepsilon_\parallel = \varepsilon_0$, which corresponds to a tubular beam in an unbounded isotropic dielectric, and $\varepsilon_\perp = \varepsilon_\parallel = \varepsilon_p$, which corresponds to a tubular beam in an unbounded isotropic plasma. In the case of a beam in a dielectric, a solution of equation (58) continuous and bounded at zero is taken in the form

$$E_z(r) = A\begin{cases} J_0(\kappa_0 r)H_0^{(1)}(\kappa_0 r_b)\,, & r < r_b\,, \\ H_0^{(1)}(\kappa_0 r)J_0(\kappa_0 r_b)\,, & r > r_b\,, \end{cases} \qquad (61)$$

where κ_0 is defined in (17) and J_0 and $H_0^{(1)}$ are the Bessel and Hankel functions of the first kind. When writing equation (61), we took into account that only beam waves will be considered, i.e., it will be $\omega \approx k_z u$. Then, for $u > c/\sqrt{\varepsilon_0}$, the quantity κ_0^2 is greater than zero. Inserting solution (61) into the matching condition (60) and eliminating the constant A, we obtain the following dispersion equation for the spectra of charge density waves of a thin tubular beam in an infinite isotropic dielectric:

$$(\omega - k_z u)^2 = -\mathrm{i}\,\frac{1}{4}\,S_b\kappa_0^2\,\frac{\omega_b^2\gamma^{-3}}{\varepsilon_0}\,J_0(\kappa_0 r_b)H_0^{(1)}(\kappa_0 r_b)\,, \quad (62)$$

where $S_b = 2\pi r_b \Delta_b$ is the cross-sectional area of the thin tubular beam. Equation (62) has much the same structure as equation (23), as can be seen from the fact that the root entering equation (23) is imaginary for $u > c/\sqrt{\varepsilon_0}$. It is therefore entirely reasonable to argue that equation (62) describes a dissipative–radiative instability of a tubular beam in an unbounded dielectric. The main difference between equations (62) and (23) is that the product of the cylindrical functions on the right-hand side of (62) is an oscillating function. Consequently, the instability increment defined by equation (62) is a nonmonotone function of k_z (Fig. 15).

In the case of an electron beam in an isotropic plasma, the quantity κ_0^2 contains the dielectric permittivity of the plasma ε_p instead of ε_0, so, for any beam velocity, $\kappa_0^2 < 0$. In this case, a solution of equation (58) should be written as

$$E_z(r) = A\begin{cases} I_0(\chi_p r)K_0(\chi_p r_b)\,, & r < r_b\,, \\ K_0(\chi_p r)I_0(\chi_p r_b)\,, & r > r_b\,, \end{cases} \qquad (63)$$

where I_0 and K_0 are the modified Bessel functions, and $\chi_p^2 = k_z^2 - \omega^2/c^2 + \omega_p^2/c^2$. Inserting solution (63) into the matching condition (60), we get the following dispersion

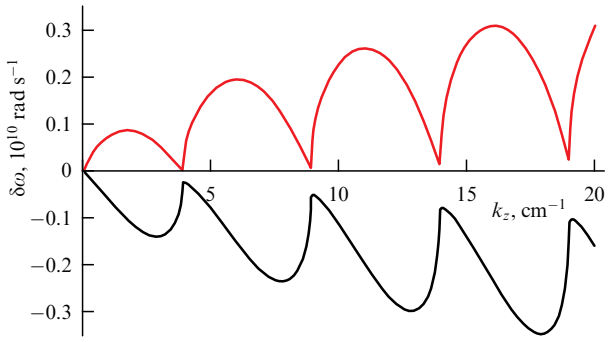

Figure 15. Complex increment of dissipative–radiative instability of a tubular beam in unbounded dielectric: $r_b = 1$ cm, $I_b = 100$ A, $\varepsilon_0 = 2$.

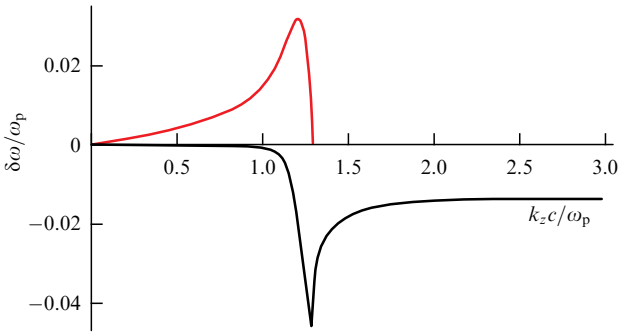

Figure 16. Complex increment of stimulated Cherenkov effect of a tubular beam in unbounded isotropic plasma: $r_b = 1$ cm, $I_b = 100$ A.

equation:

$$1 - \frac{\omega_p^2}{\omega^2} - \frac{1}{2\pi}\,S_b\chi_p^2\,\frac{\omega_{b0}^2\gamma^{-3}}{(\omega - k_z u)^2}\,I_0(\chi_p r_b)K_0(\chi_p r_b) = 0\,. \quad (64)$$

Equation (64) is practically the same as equation (29) which describes the stimulated Cherenkov effect on a longitudinal Langmuir wave in the plane case. Equation (64) describes the same effect, but in the cylindrical geometry. A complex increment, obtained by solving equation (64), is shown in Fig. 16. The curves in Fig. 16 do not differ qualitatively from the black curves in Fig. 6.

As can be seen, for a tubular beam in an unbounded isotropic dielectric and in an unbounded isotropic plasma, the cylindrical geometry does not lead to significant changes except for an oscillatory character of the increment of dissipative–radiative beam instability in a dielectric. For an anisotropic plasma and in the general case of a channel with finite size R, such a statement cannot be made. A study of the complicated dispersion equation — a cylindrical analog of equation (18) — is needed, which should be the subject of a separate study.

When applied to systems with cylindrical geometry, inequality (56) is obviously modified as

$$|\delta\omega| \gg \frac{c}{R_\infty}\,\frac{1}{\sqrt{\varepsilon_0}}\,, \qquad (65)$$

where R_∞ is the size shown in Fig. 1b. Inequality (65) requires either a larger electron density in the beam or a large transverse size of the electrodynamic system. An important characteristic of electron beams and electrodynamic systems

is the so-called limiting vacuum current [29], which becomes smaller as the transverse size R_∞ becomes larger.[19] Beams with currents above the limiting vacuum current are called high-current beams. Since the increment of beam instability is proportional to some power of the beam current, inequality (65), in particular as $R_\infty \to \infty$, allows one to attribute dissipative–radiative instabilities to high-current effects. This is consistent with our earlier statement that dissipative–radiative instabilities can be treated as instabilities under the stimulated Cherenkov effect in spatially developed systems. In high power MW electronics, spatially developed electrodynamic systems were always considered high-current systems.

8. Conclusions

To conclude this methodological note, let us try to define its place among the numerous studies devoted to high-frequency instabilities of electron beams in conditions where the frequency ω is close to the Doppler frequency **ku**, where **k** is the wavevector and **u** is the beam velocity vector. The notion of beam instability spread widely after the publication of papers [20, 30] which discovered the phenomenon of beam instability in plasmas. However, a year earlier, Ref. [31] described the phenomenon of spatial amplification of a wave propagating synchronously with an electron beam. It is believed that this paper laid the foundation for long and successful studies that led to the creation of one of the most widely used sources of electromagnetic radiation — the traveling-wave tube (TWT) [32–34]. For almost two subsequent decades, the common nature of the phenomena of beam instability in plasmas and wave amplification in a TWT was not seriously discussed. It was only after the establishment of plasma MW electronics [22–24, 35] that it became clear that the spatial wave amplification in a TWT and the temporal growth of a wave in the resonance beam instability in plasmas are based on one and the same phenomenon — the stimulated Vavilov–Cherenkov effect. It was not immediately recognized that the amplification of a wave synchronous with the beam and radiation from this wave are not equivalent notions. In gain on absorption (in dissipative beam instability), the fields of the actual beam are amplified, which are ultimately carried out of the system by the beam to the collector. And in the resonance beam instability in plasmas, plasma waves are excited, which, although they are not radiated in the strict sense because of their potential character, remain in the plasma after the electron beam has left it. In resonance beam instability in a retarding electrodynamic system of a classical TWT, the beam excites electromagnetic waves which leave the system as free radiation. In nonresonant beam instability in plasmas, the beam fields are excited by beam self-modulation in a plasma with negative dielectric permittivity and are carried together with the beam to the collector. It turns out that there is an intermediate case where the beam is modulated due to dissipation of its energy, but this dissipation is due to electromagnetic radiation being carried away. In this intermediate case, the beam fields and the radiation are localized in different regions of space, and the interaction between them takes place through the interface between these regions.

[19] Formally, for a transversely infinite system, the limiting vacuum current is zero.

This paper considers, in one way or another, all the known high-frequency instabilities of a straight monovelocity electron beam propagating along a strong external magnetic field in a laterally unbounded layered electrodynamic system. Nonresonant aperiodic beam instability in a medium with negative dielectric permittivity (a negative mass type instability) appears in connection with general formula (4), as well as in connection with the first increment in (31). The nonresonant dissipative beam instability appears in relation to general formula (5). General formulas (58) and (59) are devoted to the resonance instability of the stimulated Cherenkov effect in a dissipative system. However, the main focus in this study was devoted to the resonance instability of the stimulated Cherenkov effect in a system without dissipation and dissipative–radiative instability in an open system with energy losses by radiation. Indeed, the last two instabilities are the main ones for the propagation of an electron beam along a channel in a homogeneous isotropic dielectric medium. We considered the cases of a vacuum channel, a channel with an isotropic plasma, and a channel with an anisotropic plasma in a strong magnetic field. While in the stimulated Cherenkov effect the beam energy is spent to excite eigenwaves of the electrodynamic system, in dissipative–radiative instabilities, the beam energy is radiated out of the system to infinity by external waves. Such an irreversible energy drain from the beam manifests itself as some effective dissipation and makes the dissipative–radiative instability an analog of the usual dissipative beam instability in a system without radiation.

All instabilities considered here are contained in dispersion equation (18) and are limit cases of certain general process powered by energy release from an electron beam. Since the instability increments in these limit cases are expressed by different formulas, the instability mechanisms are of different physical natures, and this study is largely devoted to their discussion.

The author thanks I.N. Kartashova for the useful discussions and comments.

References

1. Kuzelev M V, Rukhadze A A *Sov. Phys. Usp.* **30** 507 (1987); *Usp. Fiz. Nauk* **152** 285 (1987)
2. Kuzelev M V, Rukhadze A A *Phys. Usp.* **51** 989 (2008); *Usp. Fiz. Nauk* **178** 1025 (2008)
3. Krall N A, Trivelpiece A W *Principles of Plasma Physics* (New York: McGraw-Hill, 1973); Translated into Russian: *Osnovy Fiziki Plazmy* (Moscow: Mir, 1975)
4. Kuzelev M V *Volnovye Yavleniya v Sredakh s Dispersiei* (Wave Phenomena in Media with Dispersion) (Classical Handbook of MSU) (Moscow: URSS, 2017)
5. Bogdanov V V, Kuzelev M V, Rukhadze A A *Sov. J. Plasma Phys.* **10** 319 (1984); *Fiz. Plazmy* **10** 548 (1984)
6. Alexandrov A F, Bogdankevich L S, Rukhadze A A *Principles of Plasma Electrodynamics* 1st ed. (Berlin: Springer-Verlag, 1984); Translated from Russian: *Osnovy Elektrodinamiki Plazmy* 2nd ed., revised and enlarged (Moscow: Vysshaya Shkola, 1988)
7. Arsenin V V, Timofeev A V "Neustoichivosti plazmy" ("Plasma instabilities"), in *Bol'shaya Rossiiskaya Entsiklopediya* (Big Russia Encyclopedia) Vol. 22 (Exec. Ed. S L Kravets) (Moscow: Bol'shaya Rossiiskaya Entsiklopediya, 2013) p. 533
8. Kadomtsev B B, Mikhailovskii A B, Timofeev A V *Sov. Phys. JETP* **20** 1517 (1965); *Zh. Eksp. Teor. Fiz.* **47** 2266 (1964)
9. Nezlin M V *Sov. Phys. Usp.* **19** 946 (1976); *Usp. Fiz. Nauk* **120** 481 (1976)
10. Lopukhin V M, Vedenov A A *Usp. Fiz. Nauk* **53** 69 (1954)
11. Tikhonov A N, Samarskii A A *Equations of Mathematical Physics* (Intern. Ser. of Monographs on Pure and Applied Mathematics,

Vol. 39) (New York: Dover Publ., 1990); Translated from Russian: *Uravneniya Matematicheskoi Fiziki* (Moscow: Nauka, 1972)
12. Landau L D, Lifshitz E M *Electrodynamics of Continuous Media* (Oxford: Pergamon Press, 1984); Translated from Russian: *Elektrodinamika Sploshnykh Sred* (Moscow: Nauka, 1982)
13. Kuzelev M V *Vvedenie v Fiziku Plazmy* (Introduction in Plasma Physics) (Classical Handbook of MSU) (Moscow: URSS, LENAND, 2022)
14. Kuzelev M V *Plasma Phys. Rep.* **28** 501 (2002); *Fiz. Plazmy* **28** 544 (2002)
15. Kuzelev M V, Rukhadze A A *Elektrodinamika Plotnykh Elektronnykh Puchkov v Plazme* (Electrodynamics of Dense Electron Beams in Plasma) (Moscow: Nauka, 1990)
16. Kartashov I N, Kuzelev M V *Plasma Phys. Rep.* **47** 453 (2021); *Fiz. Plazmy* **47** 428 (2021)
17. Thompson M W *Contemp. Phys.* **9** 375 (1968); Translated into Russian: *Usp. Fiz. Nauk* **99** 297 (1969)
18. Akhiezer A I, Shul'ga N F *Sov. Phys. Usp.* **25** 541 (1982); *Usp. Fiz. Nauk* **137** 561 (1982)
19. Kuzelev M V, Rukhadze A A *Phys. Usp.* **61** 748 (2018); *Usp. Fiz. Nauk* **188** 831 (2018)
20. Akhiezer A I, Fainberg Ya B *Dokl. Akad. Nauk SSSR* **69** 555 (1949)
21. Nezlin M V *Sov. Phys. Usp.* **13** 608 (1971); *Usp. Fiz. Nauk* **102** 105 (1970)
22. Bogdankevich L S, Kuzelev M V, Rukhadze A A *Sov. Phys. Usp.* **24** 1 (1981); *Usp. Fiz. Nauk* **133** 3 (1981)
23. Kuzelev M V, Rukhadze A A, Strelkov P S *Plazmennaya Relyativistskaya SVCh-Elektronika* (Relativistic Plasma MW Electronics) (Moscow: URSS, 2018)
24. Strelkov P S *Phys. Usp.* **62** 465 (2019); *Usp. Fiz. Nauk* **189** 494 (2019)
25. Kartashov I N, Kuzelev M V *J. Exp. Theor. Phys.* **131** 645 (2020); *Zh. Eksp. Teor. Fiz.* **158** 738 (2020)
26. Bugaev S P et al. *Radiotekh. Elektron.* **34** 400 (1989)
27. Cherepenin V A *Phys. Usp.* **49** 1097 (2006); *Usp. Fiz. Nauk* **176** 1124 (2006)
28. Bobylev Yu V, Kuzelev M V *Nelineinye Yavleniya pri Elektromagnitnykh Vzaimodeistviyakh Elektronnykh Puchkov s Plazmoi* (Nonlinear Phenomena in Electromagnetic Interactions of Electron Beams with Plasma) (Moscow: Fizmatlit, 2009)
29. Bogdankevich L S, Rukhadze A A *Sov. Phys. Usp.* **14** 163 (1971); *Usp. Fiz. Nauk* **103** 609 (1971)
30. Bohm D, Gross E P *Phys. Rev.* **75** 1851 (1949)
31. Lopukhin V M *Usp. Fiz. Nauk* **36** 456 (1948)
32. Trubetskov D I, Pishchik L A *Sov. J. Plasma Phys.* **15** 200 (1989); *Fiz. Plazmy* **15** 342 (1989)
33. Gulyaev Yu V, Kravchenko V F, Kuraev A A *Phys. Usp.* **47** 583 (2004); *Usp. Fiz. Nauk* **174** 639 (2004)
34. Trubetskov D I, Vdovina G M *Phys. Usp.* **63** 503 (2020); *Usp. Fiz. Nauk* **190** 543 (2020)
35. Bogdankevich L S, Rabinovich M S, Rukhadze A A *Sov. Phys. J.* **22** 1073 (1979); *Izv. Vyssh. Uchebn. Zaved. Fiz.* (10) 47 (1979)